Gene and Expression Analyses Reveal Enhanced Expression of Pericentrin 2 (*PCNT2*) in Bipolar Disorder

Ayyappan Anitha, Kazuhiko Nakamura, Kazuo Yamada, Yoshimi Iwayama, Tomoko Toyota, Nori Takei, Yasuhide Iwata, Katsuaki Suzuki, Yoshimoto Sekine, Hideo Matsuzaki, Masayoshi Kawai, Ko Miyoshi, Taiichi Katayama, Shinsuke Matsuzaki, Kousuke Baba, Akiko Honda, Tsuyoshi Hattori, Shoko Shimizu, Natsuko Kumamoto, Masaya Tohyama, Takeo Yoshikawa, and Norio Mori

Background: DISC1 has been suggested as a causative gene for psychoses in a large Scottish kindred. PCNT2 has recently been identified as an interacting partner of DISC1. In this study, we investigated the role of PCNT2 in bipolar disorder, by gene expression analysis and genetic association study.

Methods: By TaqMan real-time quantitative reverse transcriptase polymerase chain reaction (qRT-PCR), we examined the messenger RNA (mRNA) levels of PCNT2 in the postmortem prefrontal cortex of bipolar disorder ($n = 34$), schizophrenia ($n = 31$), and control subjects ($n = 32$), obtained from Stanley Array Collection. We also compared the mRNA levels of PCNT2 in the peripheral blood lymphocytes of bipolar disorder ($n = 21$), schizophrenia ($n = 21$), depression ($n = 33$), and control subjects ($n = 57$). For the association study, 23 single nucleotide polymorphisms (SNPs) were analyzed in 285 bipolar disorder patients and 287 age-and gender-matched control subjects, all of Japanese origin. The genotypes were determined by TaqMan assay.

Results: Significantly higher expression of PCNT2 was observed in the brain samples of bipolar group, compared with the control ($p = .001$) and schizophrenia ($p = .018$) groups. In the peripheral blood lymphocytes also, a significantly higher expression of PCNT2 was observed in the bipolar group, compared with the control subjects ($p = .043$). However, none of the SNPs analyzed in our study showed a significant association with bipolar disorder; a weak tendency toward association was observed for two intronic SNPs.

Conclusions: Our findings suggest that elevated levels of PCNT2 might be implicated in the pathophysiology of bipolar disorder.

Key Words: Association study, bipolar disorder, DISC1, PCNT2, peripheral blood lymphocytes, postmortem prefrontal cortex

Bipolar disorder, which is the sixth highest cause of global disability (1), affects approximately 1% of the population worldwide (2). The molecular pathophysiology of the illness has been controversial, although the contribution of genetic factors has been evidenced by family, twin, and adoption studies (3).

Disrupted-in-schizophrenia 1 (*DISC1*) has been identified as a disrupted gene by a balanced translocation (1; 11)(q42.1; q14.3) that co-segregated with major psychiatric disorders in a large Scottish kindred (4–7); the translocation carriers in the family manifested a wide spectrum of psychiatric phenotypes including schizophrenia, bipolar disorder, and recurrent major depression (4). A subsequent independent study by Devon *et al.* (8) of a Scottish family affected with schizophrenia and bipolar disorder failed to detect either co-segregation with the disease status or significant association involving any of the markers of the *DISC1* gene. Nevertheless, recent studies report the association of *DISC1* polymorphisms with schizophrenia (9–12) and with bipolar disorder (13,14). Hence, *DISC1* might be involved in the pathophysiology of only a limited subset of major psychiatric disorders.

Recently, it has been proved that DISC1 is a multifunctional protein interacting with several cytoskeletal and centrosomal proteins via distinct domains (15–19). Thus, a signaling pathway involving DISC1 and its interacting proteins rather than the DISC1 molecule per se might be involved in the pathology of major psychiatric disorders.

The fasciculation and elongation protein-zeta 1 (FEZ1) (18) and kendrin or pericentrin 2 (PCNT2) (20) have recently been identified as interacting partners of DISC1. DISC1 has been shown to participate in neurite outgrowth through its interaction with FEZ1 (18); the PCNT2-binding region of DISC1 overlaps with the region interacting with FEZ1 (20). A study by Yamada *et al.* (21) had suggested that *FEZ1* might be associated with schizophrenia in Japanese cohorts.

The *PCNT2* gene is located on 21q22.3, which has been identified as a bipolar disorder susceptibility region (22). In this study, we compared the messenger RNA (mRNA) expression levels of *PCNT2* in samples from the postmortem prefrontal cortex of bipolar disorder patients and schizophrenia patients, obtained from the Stanley Array Collection. Because lymphocytes are now considered to be a convenient and accessible alternative to brain samples for biochemical and genetic investigations of the functions of the central nervous system (CNS) (23), we further compared the mRNA levels of *PCNT2* in the periph-

From the Department of Psychiatry and Neurology (AA, KN, NT, Yal, KS, YS, MK, NM), Hamamatsu University School of Medicine; Department of Anatomy and Neuroscience (TK), Hamamatsu University School of Medicine, Hamamatsu; Laboratory of Molecular Psychiatry (KY, Yol, TT, TY), RIKEN Brain Science Institute, Saitama; The Osaka-Hamamatsu Joint Research (HM, SM, MT), Center for Child Mental Development; Department of Anatomy and Neuroscience (SM, TH, SS, NK, MT), Graduate School of Medicine, Osaka University; The 21st Century COE program (SM, TH, SS, NK, MT); Pharmacology Research Laboratory (AH), Tanabe Seiyaku, Osaka; Department of Brain Science (KM), Graduate School of Medicine and Dentistry, Okayama University, Okayama; and the Department of Anatomy and Development Neurobiology (KB), School of Medicine, Kobe University, Kobe, Japan.

Address reprint requests to Kazuhiko Nakamura, M.D., Ph.D., Department of Psychiatry and Neurology, Hamamatsu University School of Medicine, Hamamatsu, 431-3192, Japan; E-mail: nakamura@hama-med.ac.jp.

Received April 17, 2007; revised July 13, 2007; accepted July 13, 2007.

0006-3223/08/$34.00
doi:10.1016/j.biopsych.2007.07.010

Table 1. Demographic Characteristics of the Control, Schizophrenia, and Bipolar Groups Examined in Brain mRNA Analysis

Variables	Control $n = 32$	Schizophrenia $n = 31$	Bipolar $n = 34$	p
Age (yrs) (mean ± SD)	44.2 ± 7.69	42.8 ± 7.83	45.3 ± 10.5	.51[a]
Male/Female	23/9	26/8	16/18	.02[b]
Race	32 White	30 White; 1 Hispanic	33 White; 1 Black	.646[c]
Postmortem Interval (hours)	29.9 ± 13.3	31.2 ± 16.5	37.0 ± 17.7	.16[a]
Brain pH	6.63 ± .25	6.47 ± .24	6.42 ± .30	.01[a]
Lifetime Dose of Antipsychotics[d]	—	89,360 ± 10,5400	10,040 ± 22,900	.0003[e]

mRNA, messenger RNA.
[a]One-way analysis of variance.
[b]χ^2 test.
[c]Fisher's Exact test.
[d]Fluphenazine equivalents.
[e]*t* test.

eral blood lymphocytes of bipolar disorder, schizophrenia, and depression cases. Because *PCNT2* expression was found to be enhanced in bipolar disorder, we also performed an association study of *PCNT2* in bipolar disorder.

Methods and Materials

Gene Expression Analysis

Brain RNA. The RNA from the dorsolateral prefrontal cortex (DLPFC; Brodmann's area 46) was donated by The Stanley Medical Research Institute (SMRI; http://www.stanleyresearch.org/programs/brain_collection.asp) (24). The RNA from 31 schizophrenia patients, 34 bipolar disorder patients, and 32 control subjects was used for the study; demographic details of the subjects are shown in Table 1. The schizophrenia patients were medicated; among the bipolar disorder group, 24 patients were medicated, and 10 were not medicated. All the schizophrenia patients exhibited psychotic features; in the bipolar disorder group, 21 patients showed psychotic features, and 11 were not psychotic. Because the RNA samples were coded, the diagnoses of the subjects were masked while the assays were performed. The study was approved by the Ethics Committee of Hamamatsu University School of Medicine.

Lymphocyte RNA. We obtained blood samples from 21 drug-naïve schizophrenia patients, 21 medicated bipolar disorder patients, and 57 healthy control subjects. Because all the bipolar disorder patients were inevitably medicated owing to the course of the disorder, we also included samples from 33 drug-naïve major depressive patients in this study.

All the control and patient samples were of Japanese origin. Patient groups were recruited from the Hamamatsu University Hospital, Japan, during the period from April 1, 2002 to September 30, 2003. The patients were diagnosed according to the DSM-IV (25), by senior psychiatrists (NK, IY, SK); the severity of symptoms was evaluated with the Brief Psychiatric Rating Scale (BPRS) (26) for patients with schizophrenia and with the Hamilton Depression Rating Scale (HAM-D) (27) for patients with depression. All the major depressive patients belonged to the single episode category (DSM-IV-Text Revision 296.2) (28). Among the 21 bipolar disorder patients, 14 were in remission states, 2 each were in hypomanic and manic states, and 3 in depressive state. Remission for bipolar disorder patients was defined as the absence of any apparent affective symptoms for a minimum of 6 months, without recurrence (25); this was verified via a direct interview with patients along with a review of clinical records.

Although patients with schizophrenia and those with depression had, by definition, never received medication, all the patients with bipolar disorder had been taking antipsychotic drugs; their lifetime doses of antipsychotic drugs were calculated in terms of chlorpromazine equivalents. Some of the patients had been taking antidepressant drugs and/or lithium also.

The healthy control subjects consisted of the staff at the hospital and volunteers from the community; they were recruited by poster advertisements and word of mouth in and around Hamamatsu city. Demographic details of the subjects who participated in the study are shown in Table 2. All of the subjects were presented with a complete description of the study, and their written informed consent was obtained for participation. The study was approved by the Ethics Committee of Hamamatsu University School of Medicine.

Peripheral blood (20 mL) was drawn from the cubital vein into ethylenediaminetetraacetic acid (EDTA)-containing plastic

Table 2. Demographic Characteristics of the Control, Schizophrenia, Bipolar and Depression Groups Examined in Lymphocyte mRNA Analysis

Variables	Control $n = 57$	Drug-Naïve Schizophrenia $n = 21$	Medicated Bipolar $n = 21$	Drug-Naïve Depression $n = 33$	p
Age (yrs) (mean ± SD)	29.8 ± 8.11	33.1 ± 11.7	47.3 ± 16.7	36.8 ± 13.2	<.001[a]
Male/Female	46/11	14/7	10/11	23/10	.04[b]
Lifetime Dose of Antipsychotics[c]	—	—	252 ± 539	—	
Lithium	—	—	760 ± 472	—	
Antidepressants	—	—	79.8 ± 114	—	

mRNA, messenger RNA.
[a]One-way analysis of variance.
[b]χ^2 test.
[c]Chlorpromazine equivalents.

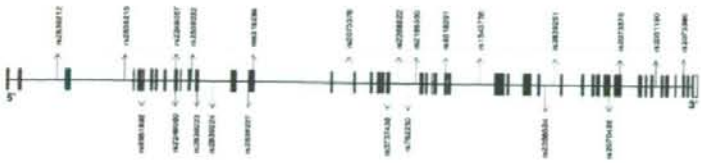

Figure 1. Genomic structure of *PCNT2*, and locations of single nucleotide polymorphisms (SNPs). Exons are indicated by boxes; SNP positions are denoted by arrows.

syringes. Lymphocytes were isolated from blood samples by the Ficoll-Paque gradient method; total RNA was extracted with RNAzolB reagent (Sawady, Tokyo, Japan), according to the manufacturer's instructions. We had been collecting blood samples at approximately the same time (10:00 AM) on the days assigned for sample collection; lymphocyte isolation and RNA extraction were done immediately thereafter. Thus, we maintained similar conditions during the collection and processing of all the samples. The RNA samples were quantified by analyzing the absorbance at 260 nm in a UV-spectrophotometer. Complementary DNA (cDNA) was synthesized by first strand reverse transcriptase reaction (RT) with Random Primer and M-MLV reverse transcriptase (Invitrogen, Carlsbad, California).

Quantitative Reverse Transcriptase Polymerase Chain Reaction. Real-time quantitative reverse transcriptase polymerase chain reaction (qRT-PCR) analysis was performed with the ABI PRISM 7900 Sequence Detection System (Applied Biosystems, Foster City, California). TaqMan primer/probes for *PCNT2* (NM_006031) and for glyceraldehyde-3-phosphate dehydrogenase (*GAPDH*; NM_002046), which served as the endogenous reference, were purchased from Applied Biosystems (Assay-on-Demand gene expression products Hs00195774 and Hs99999905, respectively). All reactions were performed in duplicate, according to the manufacturer's protocol. A comparative threshold cycle (C_T) method validation experiment was done to check whether the efficiencies of target and reference amplifications were approximately equal (the slope of the log input amount vs. $\Delta C_T < .1$). One sample was randomly chosen as the calibrator and was amplified in each plate, to correct for experimental differences among consecutive PCR runs. The amounts of *PCNT2* mRNA were normalized to the endogenous reference and expressed relative to the calibrator as $2^{-\Delta\Delta C_T}$ (comparative C_T method).

Statistical Analysis. Statistical calculations were performed with the SPSS statistical package, version 11.0.1 (SPSS, Tokyo, Japan). One-way analysis of variance (ANOVA) was used to examine the variability in the distribution of demographic variables across groups. Variability in *PCNT2* expression across the groups was analyzed with one-way ANOVA, followed by a post hoc analysis with the Tukey Honestly Significant Differences (HSD) test; to control for potential confounding factors, analysis of covariance (ANCOVA) was used. Any effect of various demographic variables upon *PCNT2* expression was examined by Pearson's correlation coefficient.

Association Study

Sample Information. We analyzed 285 bipolar disorder patients (age 48.0 ± 13.5 years [mean ± SD]; 157 male /128 female) and 287 age- and gender-matched healthy control subjects (age 48.0 ± 12.3 years, 146 male / 141 female). All the subjects were recruited from a geographical area located in the center of the mainland of Japan. Best-estimate lifetime diagnoses of patients were made by direct interview with two experienced psychiatrists, according to DSM-IV criteria (25), and with all available information from medical records, hospital staff, and family informants. Control subjects were recruited from hospital staff and company employees, documented to be free from any psychiatric problems, and were further interviewed by experienced psychiatrists to exclude any psychiatric disorders. This study was approved by the Ethics Committees of Hamamatsu University School of Medicine and RIKEN Brain Science Institute; written informed consent was obtained from all the participants.

Marker Selection. The genomic structure of *PCNT2* is based on the UCSC May 2004 draft assembly of the human genome (http://www.genome.ucsc.edu). The gene consists of 47 exons, spanning a genomic stretch of 121,587 bases (mRNA size 10,501 bases) (Figure 1). Single nucleotide polymorphisms (SNPs) for the association study were selected with the Applied Biosystems software SNPbrowser 3.5; we also referred to several databases for SNP information, including the National Centre for Biotechnology Information (NCBI dbSNP: http://www.ncbi.nlm.nih.gov/SNP) and Japanese Single Nucleotide Polymorphisms (JSNP: http://snp.ims.u-tokyo.ac.jp). On the basis of their genomic locations and minor allele frequencies (MAF > 0.1) in Japanese population, 23 SNPs were chosen for our analysis, to span the *PCNT2* gene as evenly as possible. We aimed at an average spacing of one common SNP at every 3–5 kb; however, this was not always possible, or practical. In some cases, there were long gaps with no validated common SNPs at the time we performed this study; furthermore, it was not possible to design suitable assays for some other SNPs. In addition to genotyping a common SNP at every possible 3–5 kb, we also checked the association of exonic SNPs within these intervals, to examine the possibility of *cis*-acting polymorphisms contributing to the altered expression of *PCNT2*.

Genotyping. Genomic DNA was extracted from whole blood with the QIAamp DNA blood kit (QIAGEN, Germantown, Maryland). The quality and quantity of DNA were estimated in a UV-Spectrophotometer.

Assay-on-Demand SNP genotyping products (Applied Biosystems) were used to score SNPs, on the basis of the TaqMan assay method (29). Genotypes were determined in the ABI 7900 Sequence Detection System (SDS) (Applied Biosystems) and analyzed with SDS v 2.0 software (Applied Biosystems).

Statistical Analysis. All the genotyping results were tested for Hardy-Weinberg Equilibrium (HWE). Any difference in allelic or genotypic distributions between patients and control subjects was evaluated with Fisher's exact test.

The haplotype frequencies of SNPs were estimated with the software COCAPHASE 2.403 (http://www.lithio.org/) (30). This software performs likelihood ratio tests under a logistic regression model of the probability that an allele or haplotype belongs to the case rather than the control group. The expectation maximization (EM) algorithm was used to resolve uncertain haplotypes, infer missing genotypes, and provide maximum-likelihood estimation of frequencies. Haplotype associations were also examined with this software.

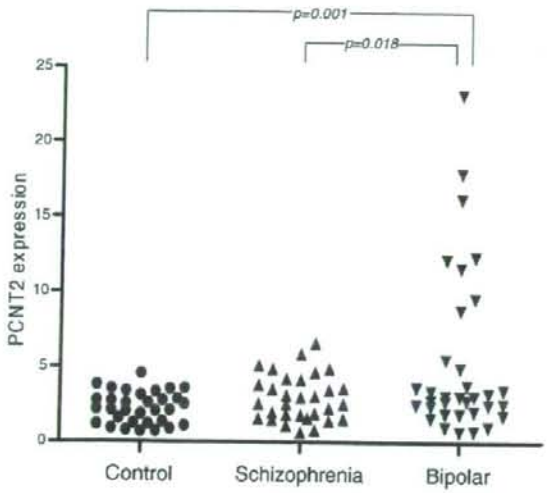

Figure 2. Post hoc pairwise comparison (Tukey Honestly Significant Differences) of *PCNT2* messenger RNA levels in the postmortem brains (Brodmann's area 46) from control, schizophrenia, and bipolar groups. A significant difference in *PCNT2* expression was observed between 1) control-bipolar (p = .001) and 2) schizophrenia-bipolar (p = .018) groups.

Results

Brain Samples

No significant difference in age [$F(2,97)$ = .69; p = .51], race distribution (Fisher's exact test p = .646), or postmortem intervals [$F(2,94)$ = 1.84; p = .16] was observed across the control, schizophrenia, and bipolar disorder groups. However, there was a significant group difference in gender distribution [$\chi^2(2)$ = 7.44, p = .02] and in brain pH [$F(2,94)$ = 5.23; p = .01] (Table 1). The control and schizophrenia groups had more men compared with the bipolar disorder group; brain pH was lower in the schizophrenia and bipolar disorder groups than that in the control group. In addition, the lifetime dose of antipsychotic drugs in the schizophrenia group was significantly higher than that in the bipolar disorder group [$t(32)$ = 4.10; p = .0003].

There was a significant difference in *PCNT2* expression across the three groups [$F(2,94)$ = 7.23; p = .001] (Figure 2). Subsequent post hoc pairwise comparison with Tukey HSD revealed a significantly higher expression of *PCNT2* in the bipolar disorder group (5.26 ± 5.47 [mean ± SD]), compared with the control (2.22 ± 1.06; p = .001) and schizophrenia (2.91 ± 1.53; p = .018) groups. The *PCNT2* expression did not differ between the control and schizophrenia groups (p = .70). After adjusting for gender and brain pH as potential confounders, with ANCOVA, the difference in *PCNT2* expression across the three groups remained significant [$F(2,92)$ = 3.77; p = .027]. The bipolar disorder group had a significantly higher expression of *PCNT2* in comparison with the control group (p = .045) but not in comparison with the schizophrenia group (p = .077). The difference in *PCNT2* expression between schizophrenia and bipolar disorder groups was significant (p = .017) when lifetime dose of antipsychotic drugs was considered as a confounding factor.

There was no significant difference [$t(30)$ = −1.114; p = .274] in *PCNT2* expression between the psychotic and non-psychotic groups of bipolar disorder patients. In addition, there was no significant difference in *PCNT2* expression [$t(32)$ = −1.71; p = .097] between the medicated and non-medicated groups of bipolar disorder patients. There were no significant correlations between *PCNT2* expression and age of onset or duration of illness, in patients with bipolar disorder.

Lymphocyte Samples

With regard to demographic characteristics, there was a significant difference in the distribution of age [$F(3,127)$ = 11.82; p < .001] and gender [$\chi^2(3)$ = 8.29; p = .04] across the control, drug-naïve-schizophrenia, medicated bipolar disorder, and drug-naïve depression groups (Table 2). The bipolar disorder group was comparatively older and had a higher proportion of women, when compared with the other three groups.

A significant difference in *PCNT2* expression was observed across the four groups [$F(3,128)$ = 6.46; p < .001] (Figure 3). Post hoc pairwise comparison with Tukey HSD showed a significantly higher expression of *PCNT2* in both the bipolar disorder group (1.14 ± .38; p = .043) and the depression group (1.22 ± .48; p = .001) than in the control group (.88 ± .32). However, *PCNT2* expression in the schizophrenia group (.93 ± .35) did not differ from and was, in effect, almost identical to that of the control group (p = .95). In addition, individuals with bipolar disorder in a remission state (1.11 ± .34) showed a significantly higher expression of *PCNT2*, compared with the control group (p = .022).

When age and gender were adjusted for as potential confounders, with ANCOVA, the difference in *PCNT2* expression across the four groups remained significant [$F(3,125)$ = 3.82; p = .003]; a significantly higher expression of *PCNT2* was observed in the bipolar disorder group (p = .010) and in the depression group (p < .001) than in the control group. Because the bipolar disorder group was, by definition, all medicated and received antipsychotic medication previously and/or at the time of the study, we examined the correlation between the lifetime dose of antipsychotic drugs and *PCNT2* expression in this group. There

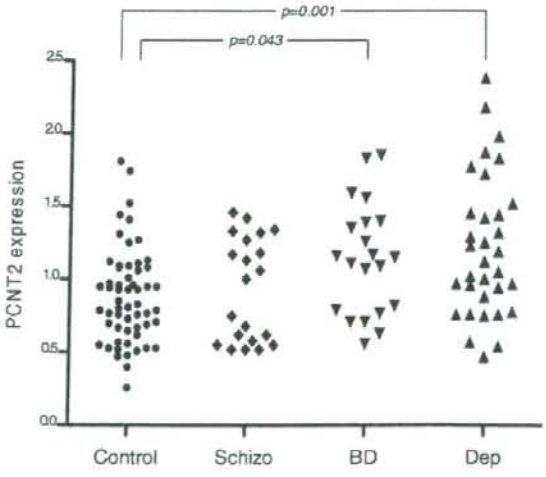

Figure 3. Post hoc pairwise comparison (Tukey Honestly Significant Differences) of *PCNT2* messenger RNA levels in the lymphocytes from control, drug-naïve schizophrenia (Schizo), medicated bipolar (BD), and drug-naïve depression (Dep) groups. A significant difference in *PCNT2* expression was observed between 1) control-bipolar (p = .043) and 2) control-dep (p = .001) groups.

Table 3. Allelic and Genotypic Distributions of PCNT2 SNPs

Marker	dbSNP ID	Samples	Allele (%)		p	Genotype (%)			p
SNP1	rs2839212		C	T		C/C	C/T	T/T	
	Intron 2	BP	428 (75.89)	136 (24.11)	.833	165 (58.51)	98 (34.75)	19 (6.74)	.515
		CT	431 (75.35)	141 (24.65)		160 (55.94)	111 (38.81)	15 (5.24)	
SNP2	rs2839215		G	A		G/G	G/A	A/A	
	Intron 3	BP	425 (75.62)	137 (24.38)	.756	163 (58.01)	99 (35.23)	19 (6.76)	.706
		CT	428 (74.83)	144 (25.17)		159 (55.59)	110 (38.46)	17 (5.94)	
SNP3	rs9981892		G	A		G/G	G/A	A/A	
	Intron 5	BP	423 (75.00)	141 (25.00)	.491	162 (57.45)	99 (35.11)	21 (7.45)	.56
		CT	439 (76.75)	133 (23.25)		168 (58.74)	103 (36.01)	15 (5.24)	
SNP4	rs2249057		C	A		C/C	C/A	A/A	
	Exon 10	BP	320 (56.74)	244 (43.26)	.985	90 (31.91)	140 (49.65)	52 (18.44)	.932
	(Silent)	CT	326 (56.79)	248 (43.21)		94 (32.75)	138 (48.08)	55 (19.16)	
SNP5	rs2249060		C	T		C/C	C/T	T/T	
	Exon 10	BP	428 (75.89)	136 (24.11)	.386	163 (57.80)	102 (36.17)	17 (6.03)	.472
	(Missense)	CT	448 (78.05)	126 (21.95)		172 (59.93)	104 (36.24)	11 (3.83)	
SNP6	rs2839222		A	G		A/A	A/G	G/G	
	Intron 12	BP	424 (75.44)	138 (24.56)	.349	163 (58.01)	98 (34.88)	20 (7.12)	.321
		CT	445 (77.80)	127 (22.20)		171 (59.79)	103 (36.01)	12 (4.20)	
SNP7	rs2839223		A	G		A/A	A/G	G/G	
	Exon 13	BP	430 (75.97)	136 (24.03)	.446	165 (58.30)	100 (35.34)	18 (6.36)	.506
	(Missense)	CT	447 (77.87)	127 (22.13)		172 (59.93)	103 (35.89)	12 (4.18)	
SNP8	rs2839224		G	A		G/G	G/A	A/A	
	Intron 13	BP	427 (75.98)	135 (24.02)	.468	165 (58.72)	97 (34.52)	19 (6.76)	.402
		CT	445 (77.80)	127 (22.20)		171 (59.79)	103 (36.01)	12 (4.20)	
SNP9	rs2839227		A	G		A/A	A/G	G/G	
	Exon 15	BP	428 (75.62)	138 (24.38)	.582	164 (57.95)	100 (35.34)	19 (6.71)	.640
	(Missense)	CT	442 (77.00)	132 (23.00)		169 (58.89)	104 (36.49)	14 (4.88)	
SNP10	rs6518289		C	T		C/C	C/T	T/T	
	Exon 15	BP	425 (75.62)	137 (24.38)	.534	164 (58.36)	97 (34.52)	20 (7.12)	.421
	(Missense)	CT	440 (77.19)	130 (22.81)		168 (58.95)	104 (36.49)	13 (4.56)	
SNP11	rs2073378		C	G		C/C	C/G	G/G	
	Intron 16	BP	428 (76.43)	132 (23.57)	.983	165 (58.93)	98 (35.00)	17 (6.07)	.74
		CT	439 (76.48)	135 (23.52)		166 (57.84)	107 (37.28)	14 (4.88)	
SNP12	rs3737438		C	T		C/C	C/T	T/T	
	Exon 21	BP	295 (51.94)	273 (48.06)	.158	79 (27.82)	137 (48.24)	68 (23.94)	.307
	(Silent)	CT	322 (56.10)	252 (43.90)		89 (31.01)	144 (50.17)	54 (18.82)	
SNP13	rs2268522		G	A		G/G	G/A	A/A	
	Intron 21	BP	407 (72.16)	157 (27.84)	.12	149 (52.84)	109 (38.65)	24 (8.51)	.126
		CT	390 (67.94)	184 (32.06)		128 (44.60)	134 (46.96)	25 (8.71)	
SNP14	rs762250		G	C		G/G	G/C	C/C	
	Intron 21	BP	407 (72.16)	157 (27.84)	.12	149 (52.84)	109 (38.65)	24 (8.51)	.126
		CT	390 (67.94)	184 (32.06)		128 (44.60)	134 (46.69)	25 (8.71)	
SNP15	rs2186350		A	G		A/A	A/G	G/G	
	Intron 21	BP	409 (72.52)	155 (27.48)	.08	150 (53.19)	109 (38.65)	23 (8.16)	.119
		CT	389 (67.77)	185 (32.23)		128 (44.60)	133 (46.34)	26 (9.06)	
SNP16	rs6518291		A	G		A/A	A/G	G/G	
	Exon 26	BP	430 (76.79)	130 (23.21)	.958	167 (59.64)	96 (34.29)	17 (6.07)	.705
	(Missense)	CT	440 (76.66)	134 (23.34)		167 (58.19)	106 (36.93)	14 (4.88)	
SNP17	rs1543756		G	A		G/G	G/A	A/A	
	Intron 27	BP	435 (76.86)	131 (23.14)	.827	169 (59.72)	97 (34.28)	17 (6.01)	.637
		CT	438 (76.31)	136 (23.69)		165 (57.49)	108 (37.63)	14 (4.88)	
SNP18	rs2268524		C	T		C/C	C/T	T/T	
	Intron 31	BP	295 (52.30)	269 (47.70)	.144	81 (28.72)	133 (47.16)	68 (24.11)	.214
		CT	325 (56.62)	249 (43.38)		90 (31.36)	145 (50.52)	52 (18.12)	
SNP19	rs2839251		C	T		C/C	C/T	T/T	
	Intron 31	BP	432 (76.33)	134 (23.67)	.83	167 (59.01)	98 (34.63)	18 (6.36)	.507
		CT	435 (75.78)	139 (24.22)		162 (56.45)	111 (38.68)	14 (4.88)	
SNP20	rs2070426		C	G		C/C	C/G	G/G	
	Exon 37	BP	410 (72.70)	154 (27.30)	.104	150 (53.19)	110 (39.01)	22 (7.80)	.107
	(Missense)	CT	392 (68.29)	182 (31.71)		128 (44.60)	136 (47.39)	23 (8.01)	

Table 3. (continued)

Marker	dbSNP ID	Samples	Allele (%)		*p*	Genotype (%)			*p*
SNP21	rs2073376		G	A		G/G	G/A	A/A	
	Exon 38	BP	410 (72.44)	156 (27.56)	.125	150 (53.00)	110 (38.87)	23 (8.13)	.107
	(Missense)	CT	392 (68.29)	182 (31.71)		128 (44.60)	136 (47.39)	23 (8.01)	
SNP22	rs2051190		T	C		T/T	T/C	C/C	
	Intron 41	BP	413 (72.71)	155 (27.29)	.102	152 (53.52)	109 (38.38)	23 (8.10)	.081
		CT	392 (68.29)	182 (31.71)		128 (44.60)	136 (47.39)	23 (8.01)	
SNP23	rs2073380		A	C		A/A	A/C	C/C	
	Exon 45	BP	293 (51.77)	273 (48.23)	.142	79 (27.92)	135 (47.70)	69 (24.38)	.225
	(Missense)	CT	322 (56.10)	252 (43.90)		88 (30.66)	146 (50.87)	53 (18.47)	

SNP, single nucleotide polymorphism; BP, bipolar; CT, control.

was no significant correlation between the lifetime dose of antipsychotic drugs and *PCNT2* expression ($r = -.066$, $p = .784$). In addition, no significant correlation was found between lithium doses and *PCNT2* expression ($r = -.349$, $p = .132$) or between antidepressant doses and *PCNT2* expression ($r = .412$, $p = .071$).

In patients with bipolar disorder and depression, there were no significant correlations between *PCNT2* expression and 1) age of onset, 2) duration of illness, or 3) HAM-D scores.

Association Study

Genotypic distributions of all the SNPs were found to be in HWE for the bipolar disorder group and its control subjects.

The allelic and genotypic frequencies of the 23 SNPs of *PCNT2* in the bipolar disorder and control groups are summarized in Table 3. None of the SNPs showed any significant difference in allelic or genotypic frequencies between the bipolar disorder and control groups. Tendencies for allelic and genotypic associations were observed for rs2186350 (SNP15) ($p = .0802$) and for rs2051190 (SNP22) ($p = .0814$), respectively. However, taking into account the multiple testing involved, these values become irrelevant. Haplotype analysis also failed to show any significant association.

Discussion

In this study, we observed a significantly higher expression of *PCNT2* in the brain and peripheral blood lymphocytes of bipolar disorder patients, when compared with the control subjects. The enhanced expression of *PCNT2* remained significant even after adjusting for the effect of various confounding variables; in addition, no correlation was observed between any of the medication doses and *PCNT2* expression. The lymphocyte samples from remission bipolar disorder patients and drug-naïve depression patients also showed elevated *PCNT2* expression. To our knowledge, this is the first study that has investigated *PCNT2* expression in the brain and peripheral blood lymphocytes of bipolar disorder patients.

Our findings lead us to hypothesize that *PCNT2* overexpression in the brain might contribute to the pathophysiology of bipolar disorder or could be the downstream result of some other aspect of the illness. PCNT2 has been proved to be essential for microtubule organization during cell division. In association with protein kinase A-anchoring proteins (AKAPs) and γ-tubulin ring complex (γ-TuRC), PCNT2 acts as a structural and regulatory scaffold at the centrosome, for those proteins that regulate cell cycle events (31–37). PCNT2 overexpression has been found to induce G2/antephase arrest of the cell cycle, followed by apoptosis, in COS cells. It has been proposed that the loss of the PCNT2-mediated anchoring mechanism due to its overexpression might elicit a checkpoint response that prevents mitotic entry and triggers apoptotic cell death (38). The exact molecular pathway involved in this process has yet to be identified. It is possible that PCNT2 overexpression might lead to some kind of apoptotic process in the brain, leading to its dysfunction. There are several studies that implicate apoptotic processes in the brain of bipolar disorder patients. At the histopathological level, striking reductions in neuronal density have been observed in the anterior cingulate cortex (ACCx) of bipolar disorder brains compared with schizophrenic brains (39). In addition, DNA fragmentation, which is a hallmark of apoptosis, has also been found to be increased in the ACCx of bipolar disorder subjects compared with schizophrenic subjects (40). Decreased glial number and density as well as decreased neuronal density have been reported in several regions of the frontal lobes, especially in the ACCx, of bipolar disorder brains (41). The recent hypothesis is that apoptosis might play a role in bipolar disorder and schizophrenia; however, considering the DNA damage, apoptosis is more likely to result in cell death in bipolar disorder patients but not in those with schizophrenia, in whom a more subtle perturbation in intracellular signaling might contribute to neuronal dysfunction (42). Abnormalities of PCNT2 can lead to defects in microtubule function, resulting in alterations in neuronal migration, axonal extension, and neurite outgrowth, thus leading to impaired neurodevelopment. Morphometric studies suggest that the pathophysiology of bipolar disorder includes anatomic abnormalities in the neural circuits interconnecting the prefrontal cortex, medial temporal lobe, and basal ganglia (43–45). In addition, recent studies provide evidence for a neurodevelopmental model of bipolar disorder, even though the effect might not be as pronounced as in the case of schizophrenia (46–52).

In this study, we found that the *PCNT2* expressions in peripheral blood lymphocytes were significantly higher in bipolar disorder and depressive patients than in control subjects. Lymphocytes are now considered to be a convenient and accessible alternative to brain samples for biochemical and genetic investigations of the functions of CNS, owing to the expression of neuroactive proteins and processes in lymphocytes and to altered lymphocyte functions in neuropsychiatric disorders; in addition, there are similarities of hormonal effects on the nervous system processes and lymphocyte physiology (23). Thus, the activity of the circulating blood leucocytes might be suggested to reflect the brain function. The expression of *PCNT2* in the peripheral blood lymphocytes might, therefore, be a useful biological marker of mood disorders.

The SMRI Online Genomics Database (http://www.stanleyresearch.org/brain/) reports reduced expression of

PCNT2 in bipolar disorder brain samples. The exact reason for this discrepancy with our results cannot be pointed out now. One possibility might be the difference of methodological procedures. The SMRI data are based on microarray analysis, whereas, our study was carried out with the TaqMan qRT-PCR method. The differences in sample processing might also have affected the results. The SMRI database reports the use of fixed and frozen tissue samples, whereas, we used the extracted RNA samples that were readily available from SMRI. *PCNT2* is reported to have approximately 20 alternate splice forms. Therefore, the probes used for the expression study might also account for the variation in results. However, our results from brain samples were concordant with that from lymphocyte *PCNT2* expression analysis, in which we again observed a significantly higher expression of *PCNT2* in the bipolar group, compared with the control subjects. Thus, we obtained consistent results with RNA samples from two different tissue sources.

Even though we observed an altered expression of *PCNT2* in the bipolar disorder samples, none of the SNPs analyzed in the study showed a significant association with bipolar disorder. The *PCNT2* gene is 121.6 kb long and consists of 47 exons; 433 SNPs are reported in the gene, of which 37 are in the coding region. In our study, we selected only those SNPs that had a MAF > .1 in the Japanese population and those for which TaqMan assays were possible; the 5′ regulatory region and other regulatory elements were not analyzed, thus precluding the definitive exclusion of *PCNT2* as a candidate gene for bipolar disorder. More SNPs in the coding and regulatory regions of the gene have to be analyzed to determine whether the altered expression of the gene can be attributed to *cis*-acting polymorphisms; it might also be possible that the expression of *PCNT2* gene is regulated by additional *trans*-acting factors. In the 21q22.3 region, multiple studies have replicated the positive linkage with bipolar disorder (53–61). In addition, reduced expression of *TRPC7* (transient receptor potential-related channels), also located in this region, has been observed in bipolar disorder-I patients (62).

In conclusion, this is the first report relating *PCNT2* with a psychiatric disorder. Our findings suggest that enhanced expression of *PCNT2* might be implicated in the pathophysiology of bipolar disorder: the levels of *PCNT2* mRNA in lymphocytes might be a useful biological marker of bipolar disorder. Further studies are required as follows: 1) an association study involving more SNPs and using samples of different ethnic origins, and 2) functional studies to elucidate the role of PCNT2 in CNS activities.

Drs. Anitha, Nakamura, and Yamada contributed equally to this work.

This work was supported by a Grant-in-Aid for Scientific Research (B) from the Ministry of Education, Culture, Sports, Science and Technology of Japan. Postmortem brain tissues were donated by the Stanley Medical Research Institute's brain collection, courtesy of Drs. Michael B. Knable, E. Fuller Torrey, Maree J. Webster, Serge Weis, and Robert H. Yolke.

We declare no conflict of interest.

1. Murray CJ, Lopez AD (1997): Global mortality, disability, and the contribution of risk factors: Global Burden of Disease Study. *Lancet* 349:1436–1442.
2. Weissman MM, Bland RC, Canino GJ, Faravelli C, Greenwald S, Hwu HG, *et al.* (1996): Cross-national epidemiology of major depression and bipolar disorder. *JAMA* 276:293–299.
3. Kato T (2001): Molecular genetics of bipolar disorder. *Neurosci Res* 40: 105–113.
4. Blackwood DH, Fordyce A, Walker MT, St Clair DM, Porteous DJ, Muir WJ (2001): Schizophrenia and affective disorders—cosegregation with a translocation at chromosome 1q42 that directly disrupts brain-expressed genes: Clinical and P300 findings in a family. *Am J Hum Genet* 69:428–433.
5. Millar JK, Wilson-Annan JC, Anderson S, Christie S, Taylor MS, Semple CA, *et al.* (2000): Disruption of two novel genes by a translocation co-segregating with schizophrenia. *Hum Mol Genet* 9:1415–1423.
6. Millar JK, Christie S, Anderson S, Lawson D, Hsiao-Wei Loh D, Devon RS, *et al.* (2001): Genomic structure and localisation within a linkage hotspot of Disrupted In Schizophrenia 1, a gene disrupted by a translocation segregating with schizophrenia. *Mol Psychiatry* 6:173–178.
7. St Clair D, Blackwood D, Muir W, Carothers A, Walker M, Spowart G, *et al.* (1990): Association within a family of a balanced autosomal translocation with major mental illness. *Lancet* 336:13–16.
8. Devon RS, Anderson S, Teague PW, Burgess P, Kipari TM, Semple CA, *et al.* (2001): Identification of polymorphisms within Disrupted in Schizophrenia 1 and Disrupted in Schizophrenia 2, and an investigation of their association with schizophrenia and bipolar affective disorder. *Psychiatr Genet* 11:71–78.
9. Callicott JH, Straub RE, Pezawas L, Egan MF, Mattay VS, Hariri AR, *et al.* (2005): Variation in DISC1 affects hippocampal structure and function and increases risk for schizophrenia. *Proc Natl Acad Sci U S A* 102:8627–8632.
10. Hennah W, Varilo T, Kestila M, Paunio T, Arajarvi R, Haukka J, *et al.* (2003): Haplotype transmission analysis provides evidence of association for DISC1 to schizophrenia and suggests sex-dependent effects. *Hum Mol Genet* 12:3151–3159.
11. Kockelkorn TT, Arai M, Matsumoto H, Fukuda N, Yamada K, Minabe Y, *et al.* (2004): Association study of polymorphisms in the 5′ upstream region of human DISC1 gene with schizophrenia. *Neurosci Lett* 368:41–45.
12. Sachs NA, Sawa A, Holmes SE, Ross CA, DeLisi LE, Margolis RL (2005): A frameshift mutation in Disrupted in Schizophrenia 1 in an American family with schizophrenia and schizoaffective disorder. *Mol Psychiatry* 10:758–764.
13. Hodgkinson CA, Goldman D, Jaeger J, Persaud S, Kane JM, Lipsky RH, Malhotra AK (2004): Disrupted in schizophrenia 1 (DISC1): Association with schizophrenia, schizoaffective disorder, and bipolar disorder. *Am J Hum Genet* 75:862–872.
14. Thomson PA, Wray NR, Millar JK, Evans KL, Hellard SL, Condie A, *et al.* (2005): Association between the TRAX/DISC locus and both bipolar disorder and schizophrenia in the Scottish population. *Mol Psychiatry* 10:657–668, 616.
15. Brandon NJ, Handford EJ, Schurov I, Rain JC, Pelling M, Duran-Jimeniz B, *et al.* (2004): Disrupted in Schizophrenia 1 and Nudel form a neurodevelopmentally regulated protein complex: Implications for schizophrenia and other major neurological disorders. *Mol Cell Neurosci* 25:42–55.
16. Ozeki Y, Tomoda T, Kleiderlein J, Kamiya A, Bord L, Fujii K, *et al.* (2003): Disrupted-in-Schizophrenia-1 (DISC-1): Mutant truncation prevents binding to NudE-like (NUDEL) and inhibits neurite outgrowth. *Proc Natl Acad Sci U S A* 100:289–294.
17. Millar JK, Christie S, Porteous DJ (2003): Yeast two-hybrid screens implicate DISC1 in brain development and function. *Biochem Biophys Res Commun* 311:1019–1025.
18. Miyoshi K, Honda A, Baba K, Taniguchi M, Oono K, Fujita T, *et al.* (2003): Disrupted-In-Schizophrenia 1, a candidate gene for schizophrenia, participates in neurite outgrowth. *Mol Psychiatry* 8:685–694.
19. Morris JA, Kandpal G, Ma L, Austin CP (2003): DISC1 (Disrupted-In-Schizophrenia 1) is a centrosome-associated protein that interacts with MAP1A, MIPT3, ATF4/5 and NUDEL: regulation and loss of interaction with mutation. *Hum Mol Genet* 12:1591–1608.
20. Miyoshi K, Asanuma M, Miyazaki I, Diaz-Corrales FJ, Katayama T, Tohyama M, Ogawa N (2004): DISC1 localizes to the centrosome by binding to kendrin. *Biochem Biophys Res Commun* 317:1195–1199.
21. Yamada K, Nakamura K, Minabe Y, Iwayama-Shigeno Y, Takao H, Toyota T, *et al.* (2004): Association analysis of FEZ1 variants with schizophrenia in Japanese cohorts. *Biol Psychiatry* 56:683–690.
22. Baron M (2002): Manic-depression genes and the new millennium: Poised for discovery. *Mol Psychiatry* 7:342–358.
23. Gladkevich A, Kauffman HF, Korf J (2004): Lymphocytes as a neural probe: Potential for studying psychiatric disorders. *Prog Neuropsychopharmacol Biol Psychiatry* 28:559–576.

24. Torrey EF, Webster M, Knable M, Johnston N, Yolken RH (2000): The Stanley foundation brain collection and neuropathology consortium. *Schizophr Res* 44:151–155.
25. American Psychiatric Association (1994): *Diagnostic and Statistical Manual of Mental Disorders, 4th ed.* Washington, DC: American Psychiatric Association.
26. Overall JE, Gorham DR (1962): The brief psychiatric rating scale. *Psychol Rep* 10:799–812.
27. Hamilton M (1960): A rating scale for depression. *J Neurol Neurosurg Psychiatry* 23:56–62.
28. American Psychiatric Association (2000): *Diagnostic and Statistical Manual of Mental Disorders*, 4th ed., *Text Revision*. Washington, DC: American Psychiatric Association.
29. Ranade K, Chang MS, Ting CT, Pei D, Hsiao CF, Olivier M, *et al.* (2001): High-throughput genotyping with single nucleotide polymorphisms. *Genome Res* 11:1262–1268.
30. Dudbridge F (2003): Pedigree disequilibrium tests for multilocus haplotypes. *Genet Epidemiol* 25:115–121.
31. Balczon R, Bao L, Zimmer WE (1994): PCM-1, A 228-kD centrosome autoantigen with a distinct cell cycle distribution. *J Cell Biol* 124:783–793.
32. Chen D, Purohit A, Halilovic E, Doxsey SJ, Newton AC (2004): Centrosomal anchoring of protein kinase C betaII by pericentrin controls microtubule organization, spindle function, and cytokinesis. *J Biol Chem* 279: 4829–4839.
33. Dictenberg JB, Zimmerman W, Sparks CA, Young A, Vidair C, Zheng Y, *et al.* (1998): Pericentrin and gamma-tubulin form a protein complex and are organized into a novel lattice at the centrosome. *J Cell Biol* 141:163–174.
34. Diviani D, Langeberg LK, Doxsey SJ, Scott JD (2000): Pericentrin anchors protein kinase A at the centrosome through a newly identified RII-binding domain. *Curr Biol* 10:417–420.
35. Doxsey SJ, Stein P, Evans L, Calarco PD, Kirschner M (1994): Pericentrin, a highly conserved centrosome protein involved in microtubule organization. *Cell* 76:639–650.
36. Kubo A, Sasaki H, Yuba-Kubo A, Tsukita S, Shiina N (1999): Centriolar satellites: Molecular characterization, ATP-dependent movement toward centrioles and possible involvement in ciliogenesis. *J Cell Biol* 147:969–980.
37. Rempel N (2001): Centrosomes as scaffolds: The role of pericentrin and protein kinase A-anchoring proteins. *Einstein Quart J Biol and Med* 18: 54–58.
38. Zimmerman WC, Sillibourne J, Rosa J, Doxsey SJ (2004): Mitosis-specific anchoring of gamma tubulin complexes by pericentrin controls spindle organization and mitotic entry. *Mol Biol Cell* 15:3642–3657.
39. Benes FM, Vincent SL, Todtenkopf M (2001): The density of pyramidal and nonpyramidal neurons in anterior cingulate cortex of schizophrenic and bipolar subjects. *Biol Psychiatry* 50:395–406.
40. Benes FM, Walsh J, Bhattacharyya S, Sheth A, Berretta S (2003): DNA fragmentation decreased in schizophrenia but not bipolar disorder. *Arch Gen Psychiatry* 60:359–364.
41. Harrison PJ (2002): The neuropathology of primary mood disorder. *Brain* 125:1428–1449.
42. Benes FM (2004): The role of apoptosis in neuronal pathology in schizophrenia and bipolar disorder. *Curr Opin Psychiatry* 17:189–190.
43. Beyer JL, Krishnan KR (2002): Volumetric brain imaging findings in mood disorders. *Bipolar Disord* 4:89–104.
44. Soares JC (2003): Contributions from brain imaging to the elucidation of pathophysiology of bipolar disorder. *Int J Neuropsychopharmacol* 6:171–180.
45. Soares JC, Mann JJ (1997): The functional neuroanatomy of mood disorders. *J Psychiatr Res* 31:393–432.
46. Blumberg HP, Kaufman J, Martin A, Charney DS, Krystal JH, Peterson BS (2004): Significance of adolescent neurodevelopment for the neural circuitry of bipolar disorder. *Ann N Y Acad Sci* 1021:376–383.
47. Cannon M, Caspi A, Moffitt TE, Harrington H, Taylor A, Murray RM, Poulton R (2002): Evidence for early-childhood, pan-developmental impairment specific to schizophreniform disorder: Results from a longitudinal birth cohort. *Arch Gen Psychiatry* 59:449–456.
48. Chen BK, Sassi R, Axelson D, Hatch JP, Sanches M, Nicoletti M, *et al.* (2004): Cross-sectional study of abnormal amygdala development in adolescents and young adults with bipolar disorder. *Biol Psychiatry* 56: 399–405.
49. Crow TJ (1995): Constraints on concepts of pathogenesis. Language and the speciation process as the key to the etiology of schizophrenia. *Arch Gen Psychiatry* 52:1011–1014; discussion 1019–1024.
50. David AS, Malmberg A, Brandt L, Allebeck P, Lewis G (1997): IQ and risk for schizophrenia: A population-based cohort study. *Psychol Med* 27: 1311–1323.
51. Harwood AJ (2003): Neurodevelopment and mood stabilizers. *Curr Mol Med* 3:472–482.
52. van Os J, Jones P, Lewis G, Wadsworth M, Murray R (1997): Developmental precursors of affective illness in a general population birth cohort. *Arch Gen Psychiatry* 54:625–631.
53. Alta VM, Liu J, Knowles JA, Terwilliger JD, Baltazar R, Grunn A, *et al.* (1999): A comprehensive linkage analysis of chromosome 21q22 supports prior evidence for a putative bipolar affective disorder locus. *Am J Hum Genet* 64:210–217.
54. Alda M (1999): Pharmacogenetics of lithium response in bipolar disorder. *J Psychiatry Neurosci* 24:154–158.
55. Detera-Wadleigh SD, Badner JA, Goldin LR, Berrettini WH, Sanders AR, Rollins DY, *et al.* (1996): Affected-sib-pair analyses reveal support of prior evidence for a susceptibility locus for bipolar disorder, on 21q. *Am J Hum Genet* 58:1279–1285.
56. Detera-Wadleigh SD, Badner JA, Yoshikawa T, Sanders AR, Goldin LR, Turner G, *et al.* (1997): Initial genome scan of the NIMH genetics initiative bipolar pedigrees: Chromosomes 4, 7, 9, 18, 19, 20, and 21q. *Am J Med Genet* 74:254–262.
57. Kaneva RP, Chorbov VM, Milanova VK, Kostov CS, Nickolov KI, Chakarova CF, *et al.* (2004): Linkage analysis in bipolar pedigrees adds support for a susceptibility locus on 21q22. *Psychiatr Genet* 14:101–106.
58. Kwok JB, Adams LJ, Salmon JA, Donald JA, Mitchell PB, Schofield PR (1999): Nonparametric simulation-based statistical analyses for bipolar affective disorder locus on chromosome 21q22.3. *Am J Med Genet* 88: 99–102.
59. Liu J, Juo SH, Terwilliger JD, Grunn A, Tong X, Brito M, *et al.* (2001): A follow-up linkage study supports evidence for a bipolar affective disorder locus on chromosome 21q22. *Am J Med Genet* 105:189–194.
60. Smyth C, Kalsi G, Curtis D, Brynjolfsson J, O'Neill J, Rifkin L, *et al.* (1997): Two-locus admixture linkage analysis of bipolar and unipolar affective disorder supports the presence of susceptibility loci on chromosomes 11p15 and 21q22. *Genomics* 39:271–278.
61. Straub RE, Lehner T, Luo Y, Loth JE, Shao W, Sharpe L, *et al.* (1994): A possible vulnerability locus for bipolar affective disorder on chromosome 21q22.3. *Nat Genet* 8:291–296.
62. Yoon IS, Li PP, Siu KP, Kennedy JL, Macciardi F, Cooke RG, *et al.* (2001): Altered TRPC7 gene expression in bipolar-I disorder. *Biol Psychiatry* 50: 620–626.

ARTICLE

A Homozygous Mutation in Human *PRICKLE1* Causes an Autosomal-Recessive Progressive Myoclonus Epilepsy-Ataxia Syndrome

Alexander G. Bassuk,[1,2,3] Robyn H. Wallace,[7] Aimee Buhr,[2] Andrew R. Buller,[1] Zaid Afawi,[8] Masahito Shimojo,[9] Shingo Miyata,[10] Shan Chen,[1] Pedro Gonzalez-Alegre,[4] Hilary L. Griesbach,[5] Shu Wu,[1] Marcus Nashelsky,[6] Eszter K. Vladar,[11,12] Dragana Antic,[11,12] Polly J. Ferguson,[1] Sebahattin Cirak,[16] Thomas Voit,[17] Matthew P. Scott,[12,13,14,15] Jeffrey D. Axelrod,[11] Christina Gurnett,[18] Azhar S. Daoud,[19] Sara Kivity,[20] Miriam Y. Neufeld,[8] Aziz Mazarib,[22] Rachel Straussberg,[21] Simri Walid,[23] Amos D. Korczyn,[24] Diane C. Slusarski,[5] Samuel F. Berkovic,[25,*] and Hatem I. El-Shanti[1,2,26]

Progressive myoclonus epilepsy (PME) is a syndrome characterized by myoclonic seizures (lightning-like jerks), generalized convulsive seizures, and varying degrees of neurological decline, especially ataxia and dementia. Previously, we characterized three pedigrees of individuals with PME and ataxia, where either clinical features or linkage mapping excluded known PME loci. This report identifies a mutation in *PRICKLE1* (also known as *RILP* for REST/NRSF interacting LIM domain protein) in all three of these pedigrees. The identified *PRICKLE1* mutation blocks the PRICKLE1 and REST interaction in vitro and disrupts the normal function of PRICKLE1 in an in vivo zebrafish overexpression system. PRICKLE1 is expressed in brain regions implicated in epilepsy and ataxia in mice and humans, and, to our knowledge, is the first molecule in the noncanonical WNT signaling pathway to be directly implicated in human epilepsy.

Introduction

More than a dozen clinico-molecular forms of progressive myoclonus epilepsy (PME) are known, including Unverricht-Lundborg disease (MIM 254800 resulting from *CSTB* mutations [MIM 601145]), Lafora disease (MIM 254780 resulting from *EPM2A* [MIM 607566] or *NHLRC1* [MIM 608072] mutations), the family of neuronal ceroid lipofuscinoses (with a variety of molecular defects including *PPT1* [MIM 256730], *CLN4* [MIM 204300], and *CLN5* [MIM 256731] mutations), and myoclonic epilepsy with ragged red fibers (MERFF [MIM 545000] with mitochondrial t-RNA mutations). Previously, we characterized three families with individuals affected with PME and ataxia but normal brain imaging, where either clinical features or linkage mapping excluded known PME loci.[1–3]

This report identifies a mutation in *PRICKLE1* (MIM 608500) in all three of these pedigrees. PRICKLE1 is part of the noncanonical or planar cell polarity (WNT/PCP) pathway, in which some WNT family members activate a β-CATENIN (*CTNNB1* [MIM 116806])-independent pathway.[4] In *Drosophila* and vertebrates, the WNT/PCP pathway likely regulates cell polarization.[5] Depleting *Prickle* genes in the zebrafish embryo alters the convergent-extension movements essential for gastrulation and disrupts normal calcium signaling.[6–8] *PRICKLE1* is part of a gene family encoding proteins containing a highly conserved PET domain, which mediates Prickle1-protein-binding interactions.[6,9–11] Prickle1 was discovered independently based on its ability to bind and functionally interact with the *RE1-SILENCING TRANSCRIPTION FACTOR* (*REST* [MIM 600571], which was thus separately named Rilp, for REST/NRSF interacting LIM domain protein), an essential regulator of neural genes.[12,13] The *PRICKLE1* mutation identified in this study is located in the PET domain and disrupts the PRICKLE1 and REST interaction in vitro and alters the normal function of PRICKLE1 in an in vivo zebrafish overexpression system.

[1]Department of Pediatrics, [2]Graduate Program in Genetics, [3]Graduate Program in Neuroscience, [4]Department of Neurology, [5]Department of Biology, [6]Department of Pathology, University of Iowa, Iowa City, IA 52242, USA; [7]Queensland Brain Institute, The University of Queensland, Brisbane 4072, Australia; [8]Department of Neurology, Tel Aviv Sourasky Medical Center and Sackler Faculty of Medicine, Tel Aviv University, Tel Aviv 64239, Israel; [9]Department of Molecular and Cellular Biochemistry, University of Kentucky, Louisville, KY 40536, USA; [10]Department of Anatomy & Neuroscience, Graduate School of Medicine, Osaka University, Osaka 565-0871, Japan; [11]Department of Pathology, [12]Department of Developmental Biology, [13]Department of Genetics, [14]Department of Bioengineering, [15]Howard Hughes Medical Institute, Stanford University School of Medicine, Stanford, CA 94305, USA; [16]Universitätskinderklinik Essen, Abteilung für Allgemeine Pädiatrie mit Schwerpunkt Neuropädiatrie, 45122 Essen, Germany; [17]Institut de Myologie Groupe Hospitalier Pitié-Salpêtrière, 75013 Paris, France; [18]Department of Neurology, Division Pediatric Neurology, Washington University School of Medicine, St. Louis, MO 63110, USA; [19]Department of Pediatrics, Jordan University of Science and Technology, Irbid 22110, Jordan; [20]Epilepsy Unit, [21]Department of Child Neurology, Schneider Children's Medical Center of Israel, Petach Tikvah 49202, Israel; [22]Kupat Holim Clalit, Nazareth 16000, Israel; [23]Department of Neurology, Western Galilee Hospital, Nahariya 22100, Israel; [24]Sieratzki Chair of Neurology, Tel Aviv University, Ramat Aviv 69978, Israel; [25]Epilepsy Research Centre and Department of Medicine, University of Melbourne (Austin Health), Heidelberg West, Victoria 3161, Australia; [26]Shafallah Medical Genetics Center, Doha, Qatar

*Correspondence: s.berkovic@unimelb.edu.au

DOI 10.1016/j.ajhg.2008.10.003.

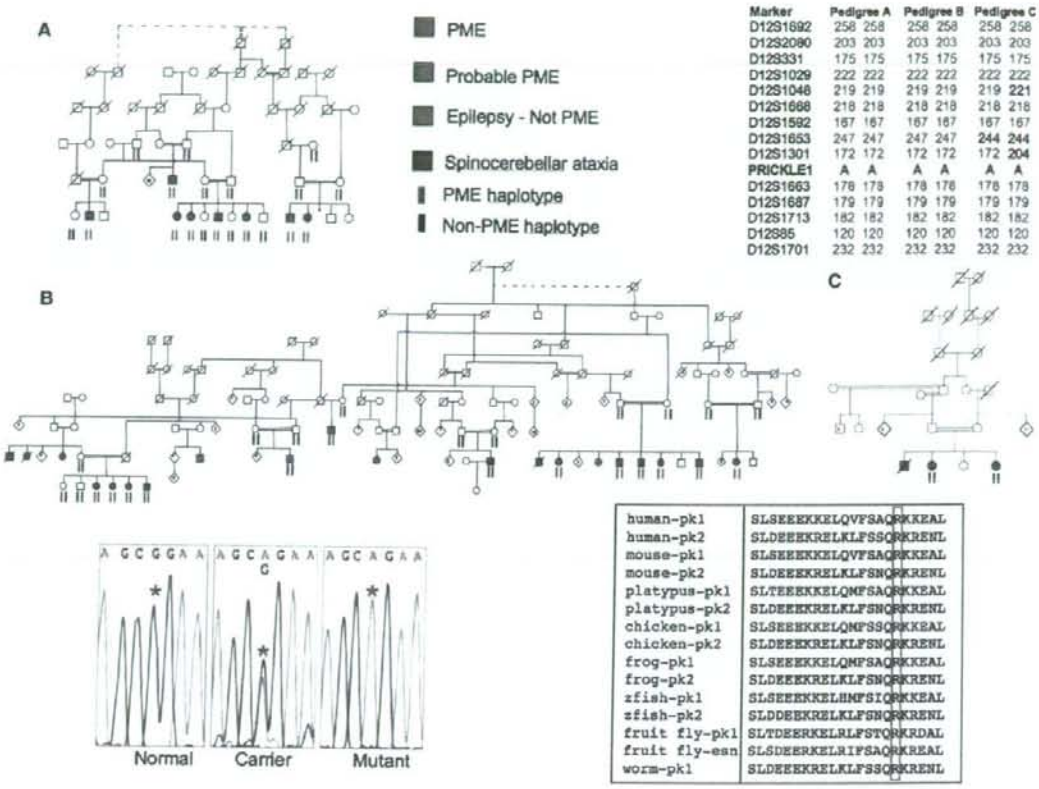

Marker	Pedigree A	Pedigree B	Pedigree C
D12S1692	258 258	258 258	258 258
D12S2080	203 203	203 203	203 203
D12S331	175 175	175 175	175 175
D12S1029	222 222	222 222	222 222
D12S1048	219 219	219 219	219 221
D12S1668	218 218	218 218	218 218
D12S1592	167 167	167 167	167 167
D12S1653	247 247	247 247	244 244
D12S1301	172 172	172 172	172 204
PRICKLE1	A A	A A	A A
D12S1663	178 178	178 178	178 178
D12S1687	179 179	179 179	179 179
D12S1713	182 182	182 182	182 182
D12S85	120 120	120 120	120 120
D12S1701	232 232	232 232	232 232

human-pk1	SLSEEEKKELQVFSAQRKKEAL
human-pk2	SLDEEEKRELKLFSSQRKRENL
mouse-pk1	SLSEEEKKELQVFSAQRKKEAL
mouse-pk2	SLDEEEKRELKLFSNQRKRENL
platypus-pk1	SLTEEEKKELQMFSAQRKKEAL
platypus-pk2	SLDEEEKRELKLFSNQRKRENL
chicken-pk1	SLSEEEKKELQMFSSQRKKEAL
chicken-pk2	SLDEEEKRELKLFSNQRKRENL
frog-pk1	SLSEEEKKELQMFSAQRKKEAL
frog-pk2	SLDEEEKRELKLFSNQRKRENL
zfish-pk1	SLSEEEKKELHMFSIQRKKEAL
zfish-pk2	SLDDEEKRELKLFSNQRKRENL
fruit fly-pk1	SLTDEERKELRLFSTQRKRDAL
fruit fly-esn	SLSDEERKELRIFSAQRKREAL
worm-pk1	SLDEEEKRELKLFSSQRKRENL

Figure 1. Pedigrees of the Affected Families, Representative Sequences, and Evolutionary Comparison of the Altered PRICKLE1 Amino Acid

Nine nuclear families from three pedigrees including 23 subjects with progressive myoclonus epilepsy and ataxia (pink symbol). Boxes on pedigrees indicate individuals previously reported by Berkovic et al.[1] (A), El-Shanti et al.[2] (B), and Straussberg et al.[3] (C). Dotted lines indicate individuals believed to be related, but the exact relationship was unknown. Subjects who probably had the familial syndrome but were not personally examined are shown in orange. Shared chromosome 12 haplotypes of affected subjects are shown on the top right. Haplotypes were remarkably stable within nuclear families and extended pedigrees. Individuals with epilepsy or ataxia, clinically distinct from the familial syndrome (green and purple symbols), did not share the haplotypes or have the *PRICKLE1* mutation. Representative DNA sequence chromograms from normal, carrier, and affected (mutant) individuals are in the bottom left panel with the red asterisks denoting the position of the abnormal nucleotide. Amino acid sequence alignment surrounding the altered amino acid for PRICKLE proteins in multiple species. pk1, Prickle1 protein; pk2, Prickle2 protein; esn, espinas protein; zfish, zebrafish. Accession numbers for the protein sequences are: human-pk1, NP_694571; human-pk2, NP_942559; mouse-pk1, NP_001028389; mouse-pk2, NP_001074615; platypus-pk1, XP_001505284; platypus-pk2, XP_001508261; chicken-pk1, XP_416036; chicken-pk2, XP_001234704; frog-pk1, NP_001016939; frog-pk-2, NP_001103517; zfish-pk1, NP_899185; zfish-pk2, NP_899186; fruit fly-pk1, NP_724534; fruit fly-esn, CAB64381; worm-pk1, NP_741435. The amino acid altered in the families and the corresponding amino acid in Prickle proteins from other species are boxed in red.

Material and Methods

Subjects

Clinical details of the three pedigrees were previously described;[1–3] pedigree B was subsequently expanded with eight more affecteds identified in three nuclear families. Clinical studies were approved by the Institutional Review Boards of the Tel Aviv Sourasky Medical Center and the Jordan University of Science and Technology. Informed consent was obtained from participating subjects and their legal guardians. The control brain specimens were obtained from a 60-year-old male with cirrhosis who died suddenly of atherosclerotic heart disease, after exemption by the Institutional Review Board of the University of Iowa and within guidelines established by Iowa statute.

Fine Mapping and Haplotyping

Microsatellite markers within the chromosome 12 pericentromeric linkage region were selected from the Marshfield human linkage map. Genotyping of 47 individuals from 3 families (Figure 1) was performed by the Australian Genome Research Facility. Marker order is based on the current human sequence map (NCBI Build 36.3).

Resequencing

PRICKLE1 amplicons (Table S2 available online) were sequenced with an automated ABI sequencer with dye terminator chemistry. After DNA amplification, unincorporated PCR primers and dNTPs in the sample were removed prior to sequencing by isolation of the desired band in a 2% agarose gel, followed by column purification. Sequences were analyzed with the computer program PHRED, which calls the bases, and PHRAP that assembled the sequence on a PC.

Control Genotyping

The 1054 individuals from the HGD-CEPH panel and the 300 Middle Eastern individuals were genotyped with the Taqman (ABI) assay on an ABI 7900 HT Fast Real Time PCR machine with the following primers according to manufacturer's instructions: PR1ex4-ex4F, GAAAAAAGAGTTGCAGGTGTTCAGT; PR1ex4-ex4R, TTAATTGTTCCTCTTCCCAGTGCTT; PR1ex4-ex4V1, VIC, CTCAGCGGAAGAAA; PR1ex4-ex4M1, FAM, CTCAGCAGAAGAAA.

The entire *PRICKLE1* gene was also directly resequenced in an additional 288 individuals, including 96 individuals of Jordanian-Palestinian ancestry.

Immunohistochemistry and Immunostaining Protocols

For mouse sections and HeLa cells, the solution used was PBS 1× Dulbecco's (pH 7.4) and the blocking solution for rabbit antibodies used was serum-free blocking media (Dako, X0909). For mouse combined with rabbit antibodies, we used M.O.M. Mouse Ig Blocking Reagent (Vector, BMK-2202); add 2 drops of stock solution to 2.5 ml of PBS. For human sections, the solution used was PBS 1X Dulbecco's (pH 7.4) and the blocking solution was serum-free blocking media (Dako, X0909).

Antibodies

Rabbit polyclonal antibody to mouse Prickle1 was produced with amino acids 808–822 by A.G.B. and with amino acids 339–514 by D.A. Specificity for Prickle1 and not Prickle2 was confirmed by immunostaining of myc-tagged cDNAs encoding Prickle1 or Prickle2 proteins into HeLa cells (data not shown). NeuN (Chemicon), GFAP (Dako), myc 9E10 (Sigma), and GFAP (Santa Cruz) antibodies were used at a 1:400–1:500 dilutions for immunohistochemistry and immunoblotting. Mouse and rabbit antibodies were diluted in M.O.M. Diluent (600 μl of protein concentrate stock solution added to 7.5 ml of PBS [Vector, BMK-2202]). Sequential rabbit antibodies were diluted in PBS 1X. Secondary antibodies were diluted 1/500 in blocking for mouse+rabbit antibodies or in PBS for rabbit antibody. We used the goat anti-rabbit IgG $(Fab')_2$-Alexa Fluor 568 conjugated antibody (Invitrogen, A21069) for the anti-GFAP antibody and the goat anti-mouse IgG $(Fab')_2$-Alexa Fluor 568 conjugated Ab (Invitrogen, A11019) for anti-NeuN antibody. We used the goat anti-rabbit IgG $(Fab')_2$-Alexa Fluor 488 conjugated Ab (Invitrogen, A11070) for the Prickle1 antibodies. The nuclear counterstain To-Pro3 (Invitrogen, T3605) was diluted 1/2000 in PBS 1X or DAPI. Slides were mounted with Vector Labs, H-1000.

Staining Protocol, Mouse Sections

Procedure. Procedures were performed at room temperature or as indicated. Sections were deparaffinized with autostainer program #3 and rehydrated with ddH_2O. To perform antigen retrieval by microwave, citrate buffer (pH 6.0) was prewarmed for ~30 s in a Teflon Coplin jar, and slides were added under the following conditions: restriction temperature, +95°C; wattage, #6 (601 W); pulse 5 min, hold 5 min (no microwave applied), pulse 5 min, then slides were left in the dish to cool to room temperature for about 20 min. Next, slides were washed in PBS 1X (pH 7.4), 3x3 min. Sections were permeabilized with 0.1% Triton X-100 in PBS for 10 min, washed in PBS 1X (pH 7.4), 3x3 min. Blocking was performed for rabbit and mouse primary antibodies together by applying the working solution of M.O.M. mouse Ig blocking reagent X1 hr, then PBS 3x3 min, then working solution M.O.M. diluent for 5 min.

Primary Antibodies. Serum-free blocking media was added for 1 hr, then primary antibodies were added at the following dilutions: rabbit anti-prickle 1 antibodies 1/250-1/375 were added with mouse anti-NeuN (Chemicon, MA13377) 1/500 or rabbit anti-prickle 1 affinity-purified antibody 1/250-1/375 was added followed by rabbit anti-GFAP Ab (Dako, Z0344) 1/1000 and stored in a slide folder at +4°C.

Sequential Stainings. The following variation was used. Sections were blocked (serum-free protein block) for 30 min, then primary antibody (anti-GFAP antibody) was added for 1 hr, then washed with PBS 1X (pH 7.4), 6 times for 3 min, and then the secondary antibody-conjugated fluorophore was added (in the dark) for 30 min. The slide was then washed with PBS 1X (pH 7.4), 6x for 3 min. Nuclear counterstain (in the dark) was then added for 5 min. Slides were then rinsed in PBS 1X and mounted in Vecta-Shield and stored in slide-folder at +4°C. Nuclei were viewed in the Far red channel (647 nm Ex). Anti-Prickle1 antibodies were viewed in the green channel (488 nm Ex), and anti-GFAP or anti-NeuN antibodies were viewed in red channel (568 nm Ex).

Staining Protocol, Human Sections

Procedure. Procedures were performed at room temperature or as indicated. Sections were deparaffinized (with an autostainer) and rehydrated with ddH_2O. Antigen retrieval was performed by microwave staining. Citrate buffer (pH 6.0) was prewarmed in the microwave for ~30 s in a Teflon Coplin jar. Slides were then added with temperature restriction: +95°C, wattage: #6 (601 W), pulse 5 min, hold 5 min (no microwave applied), pulse 5 min. Slides were then cooled to room temperature for about 20 min, washed in PBS 1X (pH 7.4), 3x for 3 min, and permeabilized with 0.1% Triton X-100 in PBS for 10 min, washed in PBS 1X (pH 7.4), 3x3 min blocked with serum-free blocking media for 1 hr. Primary antibodies were added for 1 hr, then washed with PBS, 6x for 3 min, secondary antibodies were added in the dark for 1 hr, then washed with PBS, 6x for 3 min. Slides were mounted with VectaShield and sections were stored in a slide folder at +4°C.

Primary Antibodies. Primary antibodies were diluted in PBS 1X. Rabbit anti-prickle 1 antibody 1/250-1/375 and mouse anti-NeuN (Chemicon, MA13377) 1/500 were used together, and rabbit anti-prickle 1 antibody 1/250-1/375 and rabbit anti-GFAP Ab (Dako, Z0344) 1/1000 were used sequentially. Goat anti-rabbit IgG $(Fab')_2$-Alexa Fluor 488 conjugated antibody (Invitrogen, A11070) secondary antibody was diluted 1/500 in PBS. To-Pro3 (Invitrogen, T3605) was diluted 1/2000 in PBS 1X and was used as the nuclear counterstain. Slides were mounted with VectaShield (Vector Labs, H-1000).

Sequential Stainings. After the first primary and secondary antibodies were applied, slides were blocked (serum-free protein block) for 30 min, and then the second primary antibody was applied for 1 hr, then the slides were washed in PBS 1X (pH 7.4), 6x for 3 min, and then the second secondary antibody-fluorophore conjugated was added in the dark for 30 min, and then washed in PBS 1X (pH 7.4), 6x for 3 min. Nuclear counterstain was then added (in the dark) for 5 min, and slides were rinsed with PBS

1X, and mounted in VectaShieldand and stored in a slide-folder at +4°C. Nuclei are viewed in the far red channel (647 nm Ex), anti-Prickle1 antibodies are viewed in the green channel (488 nm Ex), and anti-NeuN or GFAP antibodies are viewed in red channel (568 nm Ex).

HeLa Cell Staining

Mouse monoclonal anti-Myc 9E10 (Sigma) 1/1000 was added (EGFP viewed directly in green channel), then PBS was added 6 times for 3 min followed by secondary antibodies in the dark for 1 hr, then PBS 6 times for 3 min, and slides were then mounted with VectaShield and double labeled sections were stored with Ms + Rb Abs in slide folder at +4°C.

Confocal Microscopy

All confocal microscopy was performed on a Zeiss 510 Confocal Microscope at the University of Iowa or on a Leica confocal microscope at Stanford University. The thickness of the confocal images and all details of exposure time are embedded within the digital photographs used in this manuscript and available upon request.

Plasmids

The full-length human *PRICKLE1* cDNA in the PCR-bluntII-TOPO (Open Biosystems) was cloned into the EcoRI (5′) and XhoI (3′) sites of the pCS2+ vector, with the EGFP epitope added in-frame to the 3′ end of the gene by PCR site-directed mutagensis/chimeragnesis. The R104Q encoding mutation was introduced by site-directed mutagenesis, and the entire cDNA was resequenced after introduction of the mutation to insure that no additional mutations were introduced. Myc-REST was the same construct used previously to define the Prickle-REST interaction.[12,13]

Transfections

Transfections into HeLa cells were performed as previously described.[12,13]

Nuclear REST Measurement. To measure the impact of the PRICKLE1 mutation on the localization of REST, cells transfected with wild-type and myc-REST or mutant PRICKLE1 and myc-REST and quantified with a variation of the method previously reported.[14,15] All GFP+/myc+ cells were counted and a score of 4 was assigned for myc nuclear fluorescence much greater than myc cytoplasmic fluorescence, 3 for myc nuclear fluorescence greater than myc cytoplasmic fluorescence, 2 for myc nuclear fluorescence equal to myc cytoplasmic fluorescence, 1 for myc nuclear fluorescence less than myc cytoplasmic fluorescence, and 0 for myc nuclear fluorescence much less than myc cytoplasmic fluorescence. The mean REST nuclear score was calculated for 100 GFP+/myc+ cells in each condition.

Coimmunoprecipitations

Coimmunoprecipitations with slight variations as previously described.[12,13] In brief, myc-mouse REST and GFP-human Prickle1 plasmids were cotransfected into HeLa cells according to the Lipofectamine 2000 protocol. After 48 hr incubation, cells were lysed with 300 μl cold NET-N + Roche Protease Inhibitor. Lysates were sonicated 3 times for 4 s. 60 μl of the crude lysates were removed and mixed with 110 μl of denaturing loading buffer. The remaining lysates were precleared by adding 5 μl of anti-rabbit beads and rotating at room temperature for 20 min. The beads were removed by centrifuging samples briefly at 10,000 rpm and removing the supernatant. Precleared lysates were then mixed with 10 μl rabbit anti-GFP conjugated beads (Santa Cruz) and rotated for 2 hr at 4°C, followed by 30 min rotation at room temperature. The supernatant was removed and the beads rinsed 3 times with 500 μL of cold NET-N lysis buffer. After rinsing, 80 μl of denaturing loading buffer was added to the immunoprecipitated samples. 15 μl of IP lysates or 10 μl of crude lysates were loaded onto a 10% SDS-PAGE gel, ran for 75 min at 200V, and electroblotted overnight at 140 mA. Membrane was incubated 1:2000 anti-GFP (Roche) or anti-myc (Sigma) for 4 hr at 4°C.

PCR Conditions for Sequencing

Primers used are listed in Table S2. For exons 2–8, the mix used for PCR was: 2 μl DNA at 20 ng/μl, 2 μl 10× NH_4 reaction buffer, 2 μl dNTP (5 mM), 0.75 μl $MgCl_2$ (50 mM), 0.2 μl Biolase Taq (5 μm/μl), 0.5 μl forward primer, 0.5 μl reverse primer (20 μM per primer), add DDH2O to 20 μl. For exon 1, Invitrogen Platinum Pfx DNA polymerase was used. PCR cycling began after 10 min at 94°C as follows: (94°C, 45 s; annealing temperature, 30 s, 72°C, 45 s) ×35 cycles, followed by 72°C for 8 min, then 4°C until removed from thermocycler.

Zebrafish Constructs and Analysis

Zebrafish prickle cDNAs and wild-type and mutant (R → Q) PCR products were cloned into the Gateway vector system (Invitrogen). Both myc-tagged and untagged forms were created. Synthetic RNA was made with the mMessage machine kit (Ambion) and injected at the 1–8 cell stage. Alterations to gastrulation movements were monitored by live image capture at 20 hr postfertilization and older. Additionally, embryos were fixed at the 8–10 somite stage for whole-mount in situ hybridization with the molecular marker *MyoD*, which labels the midline as well as the developing somites. Equivalent protein expression was verified by myc-immunostaining and western blotting.

Statistical Analysis

The results of the zebrafish injections were subjected to the Fisher's exact test with the following contingency numbers: wild-type Zfsh pk1: 6 normal embryos, 36 defective embryos; mutant Zfish pk1: 20 normal embryos, 30 defective embryos; total: 26 normal embryos, 66 defective embryos.

Results

We analyzed disease features and genetics in three consanguineous Middle-Eastern pedigrees with autosomal-recessive progressive myoclonic epilepsy syndromes with ataxia[1–3] that most closely resembled Unverricht-Lundborg disease, but without mutations in *CSTB*. Pedigree A (Figure 1) from Northern Israel was originally reported as progressive myoclonus epilepsy (a new form of Unverricht-Lundborg disease; *EPM1B*) beginning between 5 and 10 years; individuals were seen in adolescence or adult life and difficulty walking prior to onset of myoclonus was reported but not directly observed.[1] Part of pedigree B was seen in Jordan when subjects were young and the impressive feature was an early-onset ataxia with later myoclonus and seizures.[2] Re-evaluation subsequently showed features of progressive myoclonus epilepsy that was also present in newly identified members of this pedigree residing in Jordan and Northern Israel. Similarly, pedigree C was initially

regarded as a predominant ataxic syndrome when children were examined in the first decade, but later re-examination showed florid progressive myoclonic epilepsy.[3] The three affected children had impaired upgaze that was also observed in some affected members of pedigrees A and B. Features of a mild sensory neuropathy seen in pedigree C were not seen in the other families.

In all three pedigrees, comprising nine nuclear families, ataxia began at 4 to 5 years and evolved into an unequivocal PME phenotype with ataxia. In many forms of PME, cognitive decline is severe and generally occurs early; however, in this disorder intellect is usually preserved. Furthermore, in all affected individuals tested, brain magnetic resonance imaging gave unremarkable results. Table 1 summarizes the clinical and molecular features compared to Unverricht-Lundborg disease.

Previous linkage analysis mapped the disease locus in pedigree A and part of pedigree B (Figure 1) to the pericentromeric region of chromosome 12.[1,2] Pedigree B was next expanded considerably, and in all three pedigrees, haplotype analysis of microsatellite markers showed an identical haplotype over 12 Mb in pedigrees A and B, whereas pedigree C shared only the distal 250,000 base pairs with pedigrees A and B (Figure 1). Pedigrees A and B shared the same family name and were thought to be distantly related but the relationship could not be established with genealogical information for 5–6 generations. Pedigree C resided in a different village, had a different family name, and elders denied a connection to the family name of pedigrees A and B and to their villages.

Resequencing the entire coding region and intron-exon boundries of 47 genes in the original linkage region (Tables S1 and S2) revealed a single, shared, missense-nucleotide change in the coding region of *PRICKLE1* in all three families (c.311G → A [R104Q]; Figure 1, bottom left). The altered amino acid in PRICKLE1 lies within the highly conserved PET domain and is invariant in evolution from humans to worms and in the related PRICKLE2 and *Drosophila* Espinas proteins (Figure 1, bottom right). This nucleotide change segregated with the clinical phenotype in all three pedigrees and was neither present in any of 1054 individuals from the CEPH-HGD control DNA samples,[16] nor found in 300 samples from unrelated Middle-Eastern individuals without epilepsy. Resequencing the entire *PRICKLE1* coding region showed no other variants in another 288 control individuals without PME (including 96 Middle-Eastern individuals).

Taken together, the high degree of conservation of the residue affected by the missense change, the absence of the identified nucleotide change in more than 1300 controls (2600 chromosomes), and the lack of other PRICKLE1 variants in nearly 300 additional controls strongly support that the *PRICKLE1* gene mutation causes this autosomal-recessive, progressive myoclonus epilepsy-ataxia syndrome.

Prickle1 is expressed in multiple brain regions throughout mouse embryonic development, including regions implicated in epilepsy such as the hippocampus, cerebral cortex, and thalamus, as well as the primitive cerebellum[17–20] (and data not shown). We performed immunohistochemical analysis with two different Prickle1-specific antibodies, each directed against a distinct epitope. In this way we also detected Prickle1 expression in the postnatal murine thalamus, hippocampus, cerebral cortex, and cerebellum (Figure 2). Costaining these tissues with the neuron-specific marker NeuN and the glia-specific marker GFAP demonstrated that Prickle1 is specifically expressed in neurons, but not in glia (Figures 2C, 2D, 2G, 2H, 2K, and 2L; cerebellum costaining not shown). Similarly, in human adult thalamus, hippocampus, cerebral cortex, and cerebellum, PRICKLE1 is in neurons rather than glia (Figure 3; GFAP staining not shown). These findings demonstrate that PRICKLE1 is expressed in multiple areas of the brain thought to be involved in generating seizures (neurons of thalamus, hippocampus, and cerebral cortex) and ataxia (cerebellar neurons).

To evaluate the functional effect of this mutation on PRICKLE1-partner protein interactions, we tested whether mutant PRICKLE1 can coimmunoprecipitate REST (Figure 4). Although, as previously described, wild-type PRICKLE1 binds REST directly,[12,13] mutant PRICKLE1 fails to bind REST in vitro. Furthermore, because REST nuclear localization is altered in brains from patients with Huntington's disease with known mutations in Huntingtin,[21] we tested whether mutant PRICKLE1 affected the subcellular localization of REST. Indeed, in HeLa cells, immunolocalization shows that whereas overexpression of wild-type PRICKLE1 results in cytoplasmic retention of REST, overexpressed mutant PRICKLE1 fails to retain REST in the cytoplasm (representative cells are shown in Figure 5A). To quantify the effect of mutant PRICKLE1 on REST nuclear localization, we counted cells based on REST expression in the cytoplasm, nucleus, or both cytoplasm and nucleus, in cells cotransfected with REST+PRICKLE1 versus REST + mutant PRICKLE1 and found significantly increased nuclear REST in cells cotransfected with mutant PRICKLE1 (Figure 5B). Therefore, the identified *PRICKLE1* mutation

Table 1. Comparison of the Progressive Myoclonus Epilepsy-Ataxia Syndrome Described Here to Classical Unverricht-Lundborg Disease

	Progresssive Myoclonus Epilepsy-Ataxia Syndrome	Unverricht-Lundborg Disease[a]
First symptom	ataxia around age 4 yr	myoclonic or tonic-clonic seizures
Seizure onset: mean	7 yr	10–11 yr
Seizure onset: range	5–10 yr	6–16 yr
Progressive features	worsening myoclonus, ataxia, impaired up-gaze	worsening myoclonus, ataxia
Cognitive decline	mild or absent	mild or absent
Mode of inheritance	autosomal recessive	autosomal recessive
Linkage	12p11–q13	21q22.3
Gene	*PRICKLE1*	*Cystatin B*

[a] Modified and updated from Berkovic et al.[1]

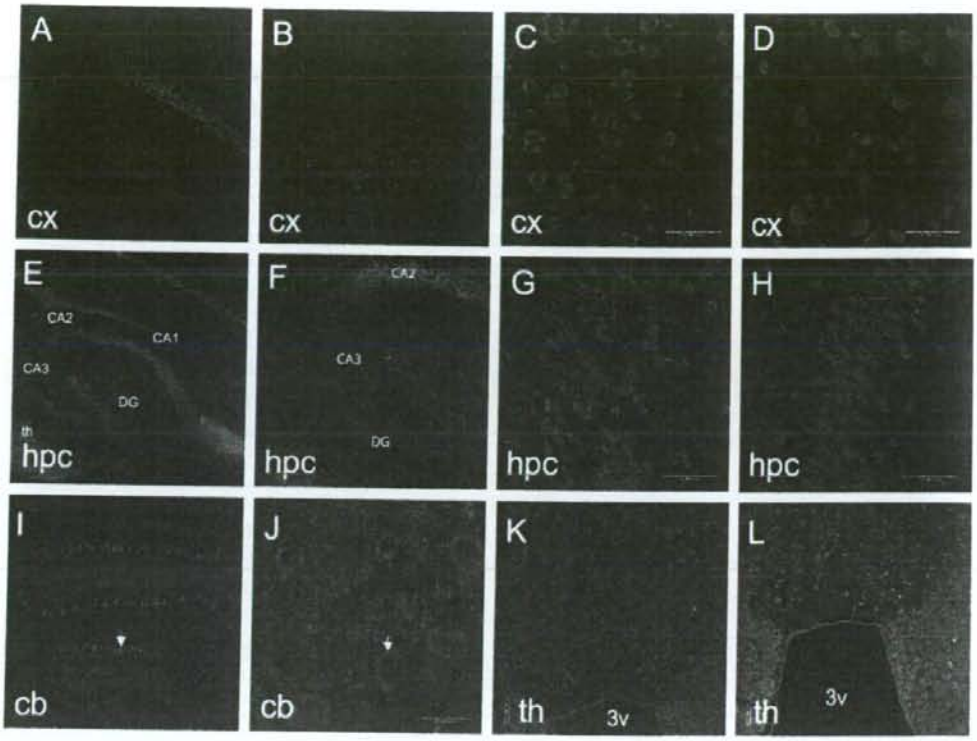

Figure 2. Expression of Prickle1 in Postnatal Mouse Brain

Prickle1 expression in cortex (A–D), hippocampus (E–H), cerebellum (I, J), and thalamus (K, L). For (A), (B), (E), (F), (I), and (J), Prickle1 antibody, raised against epitope corresponding to amino acids 339–514 of Prickle1, is labeled with green secondary, nuclear staining is in red. For (C), (D), (G), (H), (K), and (L), Prickle1 antibody, raised against epitope corresponding to amino acids 808–822 of Prickle1, is labeled in green. In (C), (D), (G), (H), (K), and (L), nuclear staining is in blue. In (C), (G), and (K), GFAP staining is in red. In (D), (H), and (L), NeuN, staining is in red. Arrows point to representative cerebellar Purkinje cells. 3v, third ventricle from coronal section; CA1, CA2, CA3, hippocampal *Cornu Ammonis* subregions; cb, cerebellum; cx, cerebral cortex; DG, dentate gyrus; hpc, hippocampus; th, thalamus. Magnification is 10× in (A), (E), and (I); 20× in (B), (F), (J), (K), and (L); 60× in (C), (D), (G), and (H). (A), (B), (E), (F), (I), and (J) are from P7 brain, (C), (D), (G), (H), (K), and (L) are from adult brain. (A)–(J) are from sagittal sections, (K) and (L) are coronal sections. A representative sample of sagittal sections from a P19 brain at multiple magnifications can be found in Figure S1.

disrupts both normal REST-binding and REST subcellular localization.

To investigate whether the mutant Prickle1 protein is functionally different from the wild-type in vivo, we injected zebrafish embryos with RNA encoding either wild-type or mutant zebrafish *prickle1*. As previously demonstrated, overexpressing wild-type *prickle1* alters gastrulation, resulting in a reduced anterior-posterior length (Figures 6A and 6B) and lateral expansion of somites (Figures 6C and 6D). Here, we further demonstrated that, compared to wild-type Prickle1, expressing similar levels of R104Q mutant Prickle1 showed a significantly less pronounced phenotype (Figure 6E). Thus in a zebrafish overexpression assay, the identified *PRICKLE1* mutation alters the in vivo function of Prickle1.

Discussion

The finding of a shared haplotype and identical PRICKLE1 mutation in three separately ascertained families of the same ethnic group with PME suggests a founder effect. The variation reported in the original three reports is explained by the differences in ages of the subjects ascertained in the earlier studies. Longitudinal assessment showed a uniform phenotype summarized in Table 1. The genealogical data and smaller ancestral haplotype found in family C suggests that this family separated earlier from the common ancestral line.

The identification of a *PRICKLE1* mutation causing this PME-ataxia syndrome raises several issues regarding the biology of PRICKLE1 and the pathophysiology of

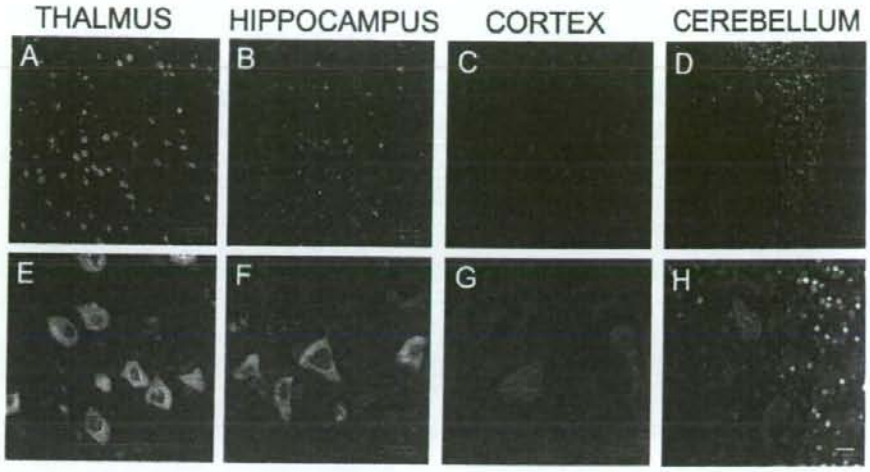

Figure 3. Expression of PRICKLE1 in Adult Human Brain
Low-power (A–D) and high-power (E–H) confocal images from immunostaining of adult human thalamus (A, E), hippocampus (B, F), cerebral cortex (C, G), and cerebellum (D, H). PRICKLE1 staining is in green, NeuN is in red, and nuclear staining is in blue. Scale markers are represented on the bottom right corner of each image.

neurological disease in these affected individuals. PRICKLE1 is part of the noncanonical or planar cell polarity (WNT/PCP) signaling pathway. In vivo studies in developing flies, frogs, and fish clearly demonstrated that Prickle1 is important for planar polarity signaling. Recently, mice lacking *Prickle1* were shown to die early in gestation, confirming an essential role for Prickle1 in development (H. Tao et al., 2008, Jap. Soc. Dev. Biol., abstract). At least some PRICKLE1 functions seem to be present in protein with the R104Q mutation because the mutation does not affect PRICKLE1 protein expression nor subcellular localization (Figure 5) and it still retains some wild-type function in our zebrafish overexpression system (Figure 6).

Our in vitro studies suggest that PRICKLE1 normally binds and translocates REST to the cytoplasm, thereby preventing REST from silencing target genes. The R104Q PRICKLE1 mutation lies within a known protein binding domain and thus disrupts REST binding (Figure 4), blocking the normal transport of REST out of the nucleus (Figure 5). These results suggest that tissues expressing mutant PRICKLE1 contain constitutively active REST which inappropriately downregulates REST target genes. This is significant because in addition to silencing neuronal genes in nonneuronal cells and neuronal precursors, REST also regulates target genes in mature neurons.[22] REST targets include ion channels and neurotransmitters, and the PME-ataxia syndrome may occur when brain regions expressing mutant PRICKLE1 misexpress these target genes. Although Prickle function was implicated in the control of cell division and morphogenesis during zebrafish neurulation[23] and REST activity was recently described in fish and frogs,[24] a role for the PRICKLE/REST interaction during neurogenesis has not yet been studied.

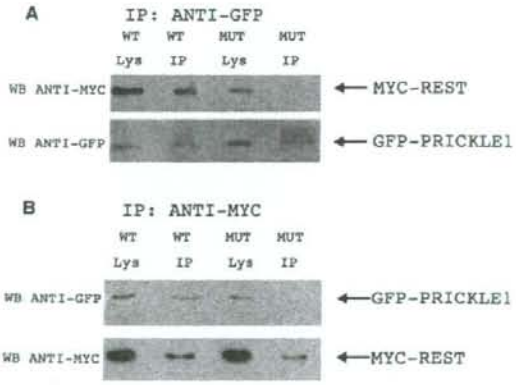

Figure 4. R104Q Mutant PRICKLE1 Has Impaired NRSF/REST Binding
Coimmunoprecipitation of REST with wild-type (WT) or R104Q mutant (MUT) encoding PRICKLE1 demonstrates decreased REST binding for MUT PRICKLE1. MYC-REST and either GFP-tagged WT or R104Q MUT PRICKLE1 plasmids were transfected into HeLa cells. Cell lysates were prepared in RIPA buffer and immunoprecipitated with agarose-conjugated anti-GFP antibody (A) or anti-MYC antibody (B). Immunoprecipitates (IP) were subjected to SDS-PAGE followed by western blotting (WB) with MYC or GFP antibodies. WB antibody noted to left of gels. The input (1/5) of immunoprecipitation is shown in the "Lys" lanes. Arrows to the right of the gels note the position of MYC-REST and GFP-PRICKLE1.

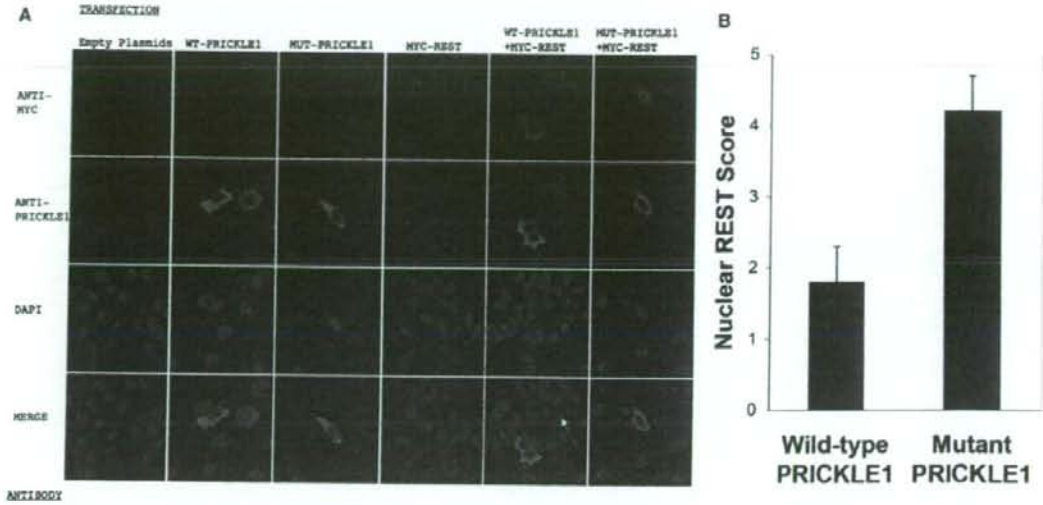

Figure 5. Subcellular Localization of Recombinant MYC-REST and WT or MUT PRICKLE1

(A) HeLa cells were transfected with MYC-REST and WT PRICKLE1 or MUT PRICKLE1, as noted on the top of the images in (A). Antibody staining with ANTI-MYC antibody (red), ANTI-PRICKLE1 antibody (green), DAPI nuclear staining (blue), and MERGED confocal images are noted on the left. Scale bar represents 9 microns. All confocal images were captured with identical exposure settings. The white arrow in the merged WT-PRICKLE1+MYC-REST marks a cell with relatively less WT PRICKLE1 expressed versus the two other WT PRICKLE1-expressing cells in the same panel. Note that increased REST in the nucleus is inversely proportional to WT PRICKLE1 expression, whereas the nuclear REST signal is strong even in the presence of a strong MUT PRICKLE1 signal (bottom right).

(B) Quantification of nuclear REST in PRICKLE1 versus mutant PRICKLE1 cotransfections. Results are the mean (± SD) of 100 cells for each group.

PRICKLE1 has also been implicated in the canonical WNT/β-catenin pathway.[25] Mutations in *EPM2A*, which cause Lafora disease—a severe form of PME with neurodegeneration—can affect the stability of the β-catenin complex in the canonical WNT/β-catenin pathway by dephosphorylating GSK3-β.[26] Although the involvement of PRICKLE1 and the influence of Epm2A on β-CATENIN may be unrelated, it is possible that a common pathway connects the effects of *PRICKLE1* mutations to Lafora disease and WNT signaling. It is notable that many affected

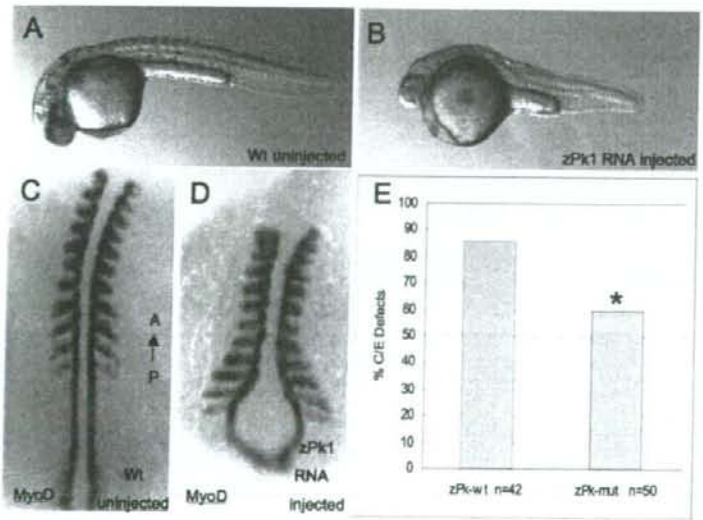

Figure 6. Mutant prickle1 Shows Decreased Activity In Vivo in Zebrafish

(A–D) Equivalent amounts of RNA encoding wild-type zebrafish *prickle1* (*pk*-wt) or zebrafish *prickle1* encoding the human R104Q homologous amino acid (*pk*-mut) were injected into zebrafish embryos and assayed for convergence extension defects by morphology (A) wild-type compared to (B) pk-overexpression, anterior to the left and with molecular markers to axial tissues in (C) wild-type and (D) pk-overexpressing embryos, anterior to the top.

(E) Decreased gastrulation defects are observed in mutant *prickle1* expressing embryos compared to wild-type *prickle* expressing embryos. The mutant Prickle1 showed significantly decreased overexpression phenotype, with a p value of 0.01 by the Fisher's exact test.

individuals with PME respond to medications such as valproic acid, which also affects the WNT/β-catenin signaling pathway through inhibition of GSK3-β.[27,28] On the other hand, valproic acid was also shown to alter inositol levels, which would interfere with calcium regulation.[29–31]

It is not yet clear how a mutation in human *PRICKLE1* leads to the PME syndrome, which is pathophysiologically characterized by increased cortical hyperexcitability with involvement of the cerebellum and probably other deep gray matter nuclei as well.

Future analysis of the effects of specific point mutations of *Prickle1* in animal models will further elucidate the molecular mechanisms underlying this PME-ataxia syndrome. Understanding the molecular and cellular basis of the disease may lead to improved diagnostic and therapeutic approaches for afflicted individuals.

Supplemental Data

Supplemental Data include one figure and two tables and can be found with this article online at http://www.ajhg.org/.

Acknowledgments

We thank the members of the families for their participation. We thank Chantal Allamargot and Kathy Walters for their assistance with immunostaining and confocal microscopy at the University of Iowa, and Kaye Suyama for her work with the antibodies at Stanford. A.G.B. is supported by NIH/NINDS grant K08NS48174. M.P.S. is an investigator of the Howard Hughes Medical Institute. D.C.S. and H.L.G. were supported by NIH CA112369. M.S. was supported by NIH/NCRR P20RR020171 and NIH MH067123. A.B. was supported by a grant from the Epilepsy Foundation. We thank Jeffrey Murray for access to the CEPH-HGD panel and for commentary on the manuscript. The authors have no disclosures and no conflicts of interest. A.G.B. wrote the manuscript, performed all immunohistochemical studies in HeLa cells and half of the tissue immunostaining, and oversaw all aspects of the resequencing, control genotyping, and coimmunoprecipitations. H.E. and A.D. clinically evaluated part of pedigree B. S.B. clinically evaluated all the pedigrees and integrated the clinical data, together with Z.A., S.K., A.K., M.N., S.W., A.Z., and R.S. H.E. and S.B. designed the mapping strategies. R.W., A.B., and S.C. performed the fine mapping, resequencing, and genotyping studies. A.B. compiled Table S1. S.C. compiled Table S2. A.R.B. performed the coimmunoprecipitations. P.F. and J.M. assisted in the design and analysis of he genotyping assays. M.N. ascertained and prepared the specimens for human tissue staining. S.W. prepared the Prickle1 antibody at the University of Iowa. P.G. assisted in the development of the cell-culture experiments. D.C.S. oversaw all zebrafish injections and analyses performed by H.L.G. M.S. provided the myc-REST construct and guidance in cell transfections. S.M. provided a mouse prickle1-GFP expression vector that was used in pilot studies in preparation for the use of a human Prickle1-EGFP construct. J.A., M.P.S., D.A., and E.K.V. produced the Prickle1 antibodies and performed the immunostaining at Stanford University.

Received: August 19, 2008
Revised: September 28, 2008
Accepted: October 3, 2008
Published online: October 30, 2008

Web Resources

The URLs for data presented herein are as follows:

Online Mendelian Inheritance in Man (OMIM), http://www.ncbi.nlm.nih.gov/Omim/
PHRAP, http://www.phroap.org

References

1. Berkovic, S.F., Mazarib, A., Walid, S., Neufeld, M.Y., Manelis, J., Nevo, Y., Korczyn, A.D., Yin, J., Xiong, L., Pandolfo, M., et al. (2005). A new clinical and molecular form of Unverricht-Lundborg disease localized by homozygosity mapping. Brain *128*, 652–658.
2. El-Shanti, H., Daoud, A., Sadoon, A.A., Leal, S.M., Chen, S., Lee, K., and Spiegel, R. (2006). A distinct autosomal recessive ataxia maps to chromosome 12 in an inbred family from Jordan. Brain Dev. *28*, 353–357.
3. Straussberg, R., Basel-Vanagaite, L., Kivity, S., Dabby, R., Cirak, S., Nurnberg, P., Voit, T., Mahajnah, M., Inbar, D., Saifi, G.M., et al. (2005). An autosomal recessive cerebellar ataxia syndrome with upward gaze palsy, neuropathy, and seizures. Neurology *64*, 142–144.
4. Ciani, L., and Salinas, P.C. (2005). WNTs in the vertebrate nervous system: from patterning to neuronal connectivity. Nat. Rev. Neurosci. *6*, 351–362.
5. Veeman, M.T., Axelrod, J.D., and Moon, R.T. (2003). A second canon. Functions and mechanisms of beta-catenin-independent Wnt signaling. Dev. Cell *5*, 367–377.
6. Carreira-Barbosa, F., Concha, M.L., Takeuchi, M., Ueno, N., Wilson, S.W., and Tada, M. (2003). Prickle 1 regulates cell movements during gastrulation and neuronal migration in zebrafish. Development *130*, 4037–4046.
7. Veeman, M.T., Slusarski, D.C., Kaykas, A., Louie, S.H., and Moon, R.T. (2003). Zebrafish prickle, a modulator of noncanonical Wnt/Fz signaling, regulates gastrulation movements. Curr. Biol. *13*, 680–685.
8. Takeuchi, M., Nakabayashi, J., Sakaguchi, T., Yamamoto, T.S., Takahashi, H., Takeda, H., and Ueno, N. (2003). The prickle-related gene in vertebrates is essential for gastrulation cell movements. Curr. Biol. *13*, 674–679.
9. Bastock, R., Strutt, H., and Strutt, D. (2003). Strabismus is asymmetrically localised and binds to Prickle and Dishevelled during *Drosophila* planar polarity patterning. Development *130*, 3007–3014.
10. Bellaiche, Y., Beaudoin-Massiani, O., Stuttem, I., and Schweisguth, F. (2004). The planar cell polarity protein Strabismus promotes Pins anterior localization during asymmetric division of sensory organ precursor cells in *Drosophila*. Development *131*, 469–478.
11. Tree, D.R., Shulman, J.M., Rousset, R., Scott, M.P., Gubb, D., and Axelrod, J.D. (2002). Prickle mediates feedback amplification to generate asymmetric planar cell polarity signaling. Cell *109*, 371–381.
12. Shimojo, M., and Hersh, L.B. (2003). REST/NRSF-interacting LIM domain protein, a putative nuclear translocation receptor. Mol. Cell. Biol. *23*, 9025–9031.
13. Shimojo, M., and Hersh, L.B. (2006). Characterization of the REST/NRSF-interacting LIM domain protein (RILP): localization and interaction with REST/NRSF. J. Neurochem. *96*, 1130–1138.

14. Galigniana, M.D., Radanyi, C., Renoir, J.M., Housley, P.R., and Pratt, W.B. (2001). Evidence that the peptidylprolyl isomerase domain of the hsp90-binding immunophilin FKBP52 is involved in both dynein interaction and glucocorticoid receptor movement to the nucleus. J. Biol. Chem. *276*, 14884–14889.
15. Gonzalez-Alegre, P., and Paulson, H.L. (2004). Aberrant cellular behavior of mutant torsinA implicates nuclear envelope dysfunction in DYT1 dystonia. J. Neurosci. *24*, 2593–2601.
16. Cann, H.M., de Toma, C., Cazes, L., Legrand, M.F., Morel, V., Piouffre, L., Bodmer, J., Bodmer, W.F., Bonne-Tamir, B., Cambon-Thomsen, A., et al. (2002). A human genome diversity cell line panel. Science *296*, 261–262.
17. Crompton, L.A., Du Roure, C., and Rodriguez, T.A. (2007). Early embryonic expression patterns of the mouse Flamingo and Prickle orthologues. Dev. Dyn. *236*, 3137–3143.
18. Katoh, M. (2003). Identification and characterization of human PRICKLE1 and PRICKLE2 genes as well as mouse Prickle1 and Prickle2 genes homologous to *Drosophila* tissue polarity gene prickle. Int. J. Mol. Med. *11*, 249–256.
19. Okuda, H., Miyata, S., Mori, Y., and Tohyama, M. (2007). Mouse Prickle1 and Prickle2 are expressed in postmitotic neurons and promote neurite outgrowth. FEBS Lett. *581*, 4754–4760.
20. Tissir, F., and Goffinet, A.M. (2006). Expression of planar cell polarity genes during development of the mouse CNS. Eur. J. Neurosci. *23*, 597–607.
21. Zuccato, C., Tartari, M., Crotti, A., Goffredo, D., Valenza, M., Conti, L., Cataudella, T., Leavitt, B.R., Hayden, M.R., Timmusk, T., et al. (2003). Huntingtin interacts with REST/NRSF to modulate the transcription of NRSE-controlled neuronal genes. Nat. Genet. *35*, 76–83.
22. Palm, K., Belluardo, N., Metsis, M., and Timmusk, T. (1998). Neuronal expression of zinc finger transcription factor REST/NRSF/XBR gene. J. Neurosci. *18*, 1280–1296.
23. Ciruna, B., Jenny, A., Lee, D., Mlodzik, M., and Schier, A.F. (2006). Planar cell polarity signalling couples cell division and morphogenesis during neurulation. Nature *439*, 220–224.
24. Olguin, P., Oteiza, P., Gamboa, E., Gomez-Skarmeta, J.L., and Kukuljan, M. (2006). RE-1 silencer of transcription/neural restrictive silencer factor modulates ectodermal patterning during *Xenopus* development. J. Neurosci. *26*, 2820–2829.
25. Chan, D.W., Chan, C.Y., Yam, J.W., Ching, Y.P., and Ng, I.O. (2006). Prickle-1 negatively regulates Wnt/beta-catenin pathway by promoting Dishevelled ubiquitination/degradation in liver cancer. Gastroenterology *131*, 1218–1227.
26. Liu, Y., Wang, Y., Wu, C., and Zheng, P. (2006). Dimerization of Laforin is required for its optimal phosphatase activity, regulation of GSK3beta phosphorylation, and Wnt signaling. J. Biol. Chem. *281*, 34768–34774.
27. Chen, G., Huang, L.D., Jiang, Y.M., and Manji, H.K. (1999). The mood-stabilizing agent valproate inhibits the activity of glycogen synthase kinase-3. J. Neurochem. *72*, 1327–1330.
28. Wiltse, J. (2005). Mode of action: inhibition of histone deacetylase, altering WNT-dependent gene expression, and regulation of beta-catenin–developmental effects of valproic acid. Crit. Rev. Toxicol. *35*, 727–738.
29. Galit, S., Shirley, M., Ora, K., Belmaker, R.H., and Galila, A. (2007). Effect of valproate derivatives on human brain myo-inositol-1-phosphate (MIP) synthase activity and amphetamine-induced rearing. Pharmacol. Rep. *59*, 402–407.
30. Shimshoni, J.A., Dalton, E.C., Jenkins, A., Eyal, S., Ewan, K., Williams, R.S., Pessah, N., Yagen, B., Harwood, A.J., and Bialer, M. (2007). The effects of central nervous system-active valproic acid constitutional isomers, cyclopropyl analogs, and amide derivatives on neuronal growth cone behavior. Mol. Pharmacol. *71*, 884–892.
31. Tokuoka, S.M., Saiardi, A., and Nurrish, S.J. (2008). The mood stabilizer valproate inhibits both inositol- and diacylglycerol-signaling pathways in *Caenorhabditis elegans*. Mol. Biol. Cell *19*, 2241–2250.

Neuroscience Letters 445 (2008) 162–165

Contents lists available at ScienceDirect

Neuroscience Letters

journal homepage: www.elsevier.com/locate/neulet

PRMT1 and Btg2 regulates neurite outgrowth of Neuro2a cells

Shingo Miyata [a,b,*], Yasutake Mori [a], Masaya Tohyama [a,b]

[a] Department of Anatomy and Neuroscience, Graduate School of Medicine, Osaka University, 2-2 Yamadaoka, Suita, Osaka 565-0871, Japan
[b] Department of Clinical Disorder Research, The Osaka-Hamamatsu Joint Research Center For Child Mental Development, 2-2 Yamadaoka, Suita, Osaka 565-0871, Japan

ARTICLE INFO

Article history:
Received 26 June 2008
Received in revised form 15 August 2008
Accepted 19 August 2008

Keywords:
PRMT1
Btg2
Neurite outgrowth
Neuro2a cells
Arginine methylation

ABSTRACT

Neurite outgrowth is one of the crucial events in the formation of neural circuits. The majority of studies on neurite outgrowth have focused on signal transduction processes based on phosphorylation and acetylation; a few studies have suggested the involvement of other molecular mechanisms. Recent progress in understanding the nature of protein arginine *N*-methyltransferases (PRMTs) raises the possibility of the involvement of protein methylation accompanied by cell shape changes during neuronal differentiation. Here, we show that PRMT1 play a pivotal role in the neurite outgrowth of Neuro2a cells. Our results revealed that PRMT1 depletion specifically affected neurite outgrowth but not the physiological processes involved in cell growth and differentiation. Furthermore, we demonstrated that Btg2, one of the PRMT1 binding partner, depletion down-regulated arginine methylation in the nucleus and inhibited neurite outgrowth. These results indicate that protein arginine methylation by PRMT1 in the nucleus is an important step in neuritogenesis.

Neurite outgrowth is extremely important for the formation of neural circuits during the developmental stage, and the reformation of neurite outgrowth plays an essential role in intractable neurodegenerative disorders [9,15]. Furthermore, most studies on neurite outgrowth have focused on signal transduction processes such as phosphorylation and acetylation [7,11,12,16]. Although the functional significance of protein methylation in nonneuronal cells has been proposed [1,2,19,18,21], its significance in neuronal cells is unknown. Recently, several studies indicated that the function of protein methylation in neuron-like cells is that arginine *N*-methylation that may cause neurite outgrowth [4–6]; however the molecular mechanism underlying this process remains unclear.

It is known that the Btg2 protein can bind to PRMT1 and increasing PRMT1 activity [14]. Furthermore, it has been reported that Btg2 is related to neuronal differentiation [8]. In this study, we demonstrate that PRMT1 is necessary for neurite outgrowth, and Btg2 expression may regulate protein arginine methylation by PRMT1 in the nucleus of Neuro2a cells by using the transient PRMT1 depletion method.

Neuro2a cells (IF050081) were obtained from the Human Science Research Resources Bank (HSRRB). These cells were maintained in Dulbecco's modified Eagle's medium (DMEM) (Invitrogen Co.) containing 10% heat-inactivated fetal bovine serum (FBS) at 37 °C in an atmosphere of 95% air/5% CO_2. For the neurite outgrowth studies, Neuro2a cells (5×10^5 cells) were cultured in DMEM containing 0.1% bovine serum albumin (BSA). When cells attained a length greater than two cell diameters they were scored for the production of outgrowths. The number of neurite-bearing cells was expressed as a percentage of the total cell number (>50 μm; three independent experiments, 300 cells each).

In order to investigate the functions of well-studied protein arginine methyltransferase, PRMT1, on the neurite outgrowth of Neuro2a cells, we first examined the effects of PRMT1 depletion from the cells by an RNA interference (RNAi)-based knockdown method. Stealth siRNA against PRMT1 (5′-AUAGGAGUCAAAGUAGUAGUCUUUG-3′), and negative control duplexes (scrambled siRNA for PRMT1, 5′-CAAAUCACAUCGUUUCUCACGAUAU-3′) were provided by Invitrogen Co. The Neuro2a cells were transfected with 100 pM of each siRNA and a mixture of scrambled siRNA by using Lipofectamine RNAiMAX (Invitrogen Co.) according to the manufacturer's instructions. Western blot analysis also demonstrated that the expression of endogenous PRMT1 in Neuro2a cells was extinguished by the PRMT1 siRNA (Fig. 1A). PRMT1-targeted siRNA significantly reduced the endogenous PRMT1 level with almost no effect on the CARM1 level (PRMT1 and CARM1 antibodies, 1:1000; Upstate Biotech) (PRMT1, 0.13 ± 0.18; CARM1, 0.98 ± 0.05) (Fig. 1A). Similarly, previous studies demonstrated that PRMT1-

Abbreviations: Btg2, B-cell translocation gene 2; BSA, bovine serum albumin; FBS, fetal bovine serum; NGF, nerve growth factor; PRMT1, protein arginine *N*-methyltransferase 1; siRNA, small interfering RNA; YFP, yellow fluorescent protein.

* Corresponding author at: Department of Anatomy and Neuroscience, Graduate School of Medicine, Osaka University, 2-2 Yamadaoka, Suita, Osaka 565-0871, Japan.
E-mail address: smiyata@anat2.med.osaka-u.ac.jp (S. Miyata).

0304-3940/$ – see front matter © 2008 Elsevier Ireland Ltd. All rights reserved.
doi:10.1016/j.neulet.2008.08.065

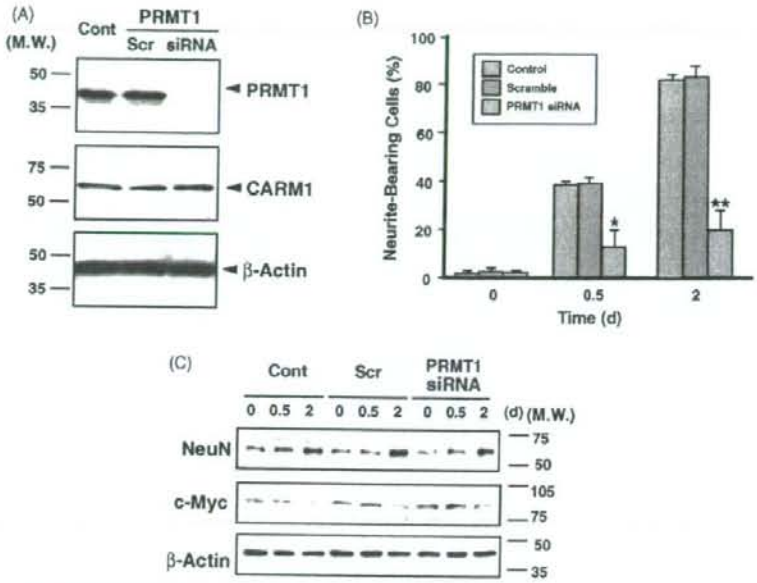

Fig. 1. Effects of PRMT1 knockdown on neurite outgrowth and differentiated neuronal phenotypes of Neuro2a cells. (A) Data representing the western blot analysis of PRMT1, CARM1, and β-actin protein expression 3 days after transfection with scrambled, or PRMT1-siRNA. Cont, nontransfected cells; Scr, scrambled siRNA-transfected cells. M.W., molecular weight. (B) Quantification of the neurite outgrowth levels of the PRMT1 depletion Neuro2a cells. The results are expressed as the mean ± S.E.M. of three independent experiments. The asterisks (*) indicate the significant effects of a decrease in the number of neurite-bearing cells (Student's *t*-test; $^{*}P < 0.05$, $^{**}P < 0.01$). (C) Changes in the expression levels of the neuronal marker NeuN and the cell proliferation markers c-Myc in the PRMT1 siRNA-transfected cells after serum withdrawal. The total cell lysate was subjected to western blot analysis by using the anti-NeuN, anti-c-Myc, or anti-β-actin antibodies. M.W., molecular weight; d, days.

targeted siRNA specifically reduced endogenous PRMT1 expression to 10–20% [10,13]. Therefore, the employed sequence of double-stranded siRNA effectively suppressed the expression of the PRMT1 genes in Neuro2a cells.

To elucidate a functional significance of protein arginine methylation, we examined the effect of PRMT1 depletion on the neuritogenesis of Neuro2a cells induced by serum deprivation. Three days after Neuro2a cells were transfected with scrambled or PRMT1-targeted siRNA were counted as neurite-bearing cells (Fig. 1B). In the growth media containing 10% fetal bovine serum , the scrambled, PRMT1-targeted siRNAs did not induce neurite outgrowth 2 days after the transfection (data not shown). Serum deprivation caused significant neurite outgrowth in the scrambled siRNA-transfected group (data not shown), while transfection with PRMT1-targeted siRNA reduced the neurite-bearing population to 20% of that observed with transfection with scrambled siRNA under the same condition (scrambled siRNA, 85.3% ± 5.2%; PRMT1 siRNA, 21.7% ± 8.6%) (Fig. 1B).

The immunodetection was performed using the ECL Western blotting detection system (GE Healthcare Bio-Science) with peroxidase-coupled secondary antibody according to the manufacturer's instructions. Interestingly enough, this siRNA-transfected cells showed an enhancement in the neuronal marker protein NeuN (1:1000; Chemicon International Inc.) 2 days after serum deprivation, while c-Myc (1:1000; Sigma–Aldrich), a proliferating marker protein, was gradually reduced (Fig. 1C). These results demonstrated that PRMT1 depletion specifically affected neurite outgrowth but not the physiological processes involved in cell growth and differentiation.

To confirm whether the reintroduction of PRMT1 into its siRNA-transfected cells reverted the knockdown phenotype, 3 days after the scrambled or PRMT1 siRNA transfection, a PRMT1 construct harboring some neutral mutations along the siRNA oligonucleotide sequence was retransfected into the Neuro2a cells. The siRNA-resistant mutant PRMT1 was visualized by the fused yellow fluorescent protein (YFP) in its N-terminus. We performed a western blot analysis and immunocytochemistry of the YFP-fused siRNA-resistant mutant PRMT1 protein expression. This fusion protein and mock YFP proteins were transiently expressed in Neuro2a cells (Fig. 2A and B), and the anti-GFP polyclonal antibody (1:1000; Abcam Ltd.) recognized either of the two proteins with expected sizes of 25 and 65 kDa, respectively (Fig. 2D). Furthermore, the anti-PRMT1 polyclonal antibody recognized only the YFP-fused siRNA-resistant mutant PRMT1 protein (Fig. 2D). Thus, we used this fusion protein to perform the subsequent experiments. The overexpressed mutant PRMT1 in the siRNA-transfected cells elevated the population of neurite-bearing cells by 2.5-fold compared to the control YFP protein (cells cultured for 2 days in the differentiation medium; YFP, 12.2% ± 2.3%; YFP-fused PRMT1, 28.2% ± 5.3%) (Fig. 2C). These findings demonstrated that arginine methylation induced by the PRMT1 protein was deeply linked to the neurite outgrowth of Neuro2a cells.

Since Btg2 was reported to be one of the interacting partners screened by the two-hybrid method using PRMT1 as bait [14], we examined the effects of the depletion of Btg2 from Neuro2a cells on the level of methylated proteins and neurite extension. Stealth siRNA against Btg2 (5′-UGUAAUGAUCGGUCAGUGCGUCCUG-3′) and negative control duplexes (scrambled siRNA for Btg2, 5′-CAGCGCACUGACCGAUCAUUGAACA-3′) were provided by Invitrogen Co. Real-time PCR was performed on an ABI PRISM 7900HT Sequence Detection System using the SYBR GREEN PCR Master Mix (Applied Biosystems). To quantify Btg2 expression levels the following primers were used: forward, 5′-ATGAGCCACGGGAAGAGAAC-3′; reverse, 5′-